Marine and Petroleum Geology 122 (2020) 104642

Contents lists available at ScienceDirect

Marine and Petroleum Geology

journal homepage: www.elsevier.com/locate/marpetgeo

Research paper

Paleozoic-Mesozoic tectono-sedimentary evolution and magmatism of the Egersund Basin area, Norwegian central North Sea

Mohsen Kalani [*,1], Jan Inge Faleide, Roy Helge Gabrielsen

Department of Geosciences, University of Oslo, P.O. Box 1047, Blindern, 0316, Oslo, Norway

ARTICLE INFO

Keywords:
Central north sea
Egersund basin
Structural grain
Seismic interpretation
Magmatism
Pre-permian
Sub-rotliegend

ABSTRACT

This study focuses on the tectonic evolution of the greater Egersund Basin in the Norwegian central North Sea, with special emphasis on Late Paleozoic extensional tectonics following Caledonian collapse and the Variscan Orogeny, and the impact of the basement structural grain on this evolution. The Caledonian collapse likely resulted in development/rejuvenation of the deepest E-W trending structures/depocenters by Late Devonian time. Thus, a late Devonian-?early Carboniferous age can be assigned to the initial extension, which was associated with the development of an E-W striking basin system, to be overprinted by N–S extensional structures of similar age. A phase of regional magmatism at the Carboniferous-Permian transition (≈300 Ma) may be associated with a large igneous province centred on the Skagerrak area. Faulting during late Carboniferous-early Permian was minor within the study area as reflected by uniform sedimentary thicknesses of the uppermost Carboniferous and lower Permian sequences. Major normal faults, mainly trending N–S, were active during a late Permian-Early Triassic rift phase affecting large parts of the central and northern North Sea area. A later phase of extension was initiated in late Middle Jurassic time and the Egersund Basin proper formed during the Late Jurassic-Early Cretaceous. The depocenters that developed during this phase was influenced by the deep Late Paleozoic (sub-salt) structural grain, including strike-slip movements along the Sorgenfrei-Tornquist Zone. Later events include mild inversion along the northern flank of the Egersund Basin, possibly as a Late Cretaceous response to far-field Alpine compression, and Cenozoic regional tilting.

1. Introduction

The influence of the basement fabric and fault populations (Proterozoic and Caledonian), referred here as the structural grain, on the development of the basin system of the Norwegian Shelf has long been debated (e.g. Bartholomew et al., 1993; Blundell et al., 1991; Donato and Tully, 1982; Færseth et al., 1995; Gabrielsen and Ramberg, 1979; Gabrielsen, 1984; Smethurst, 2000; Stewart et al., 1992; Ziegler, 1990). This discussion has been hampered by high-quality deep seismic reflection data being scarse. Although such data exist for many parts of the North Sea (e.g. Blundell et al., 1991; Christiansson et al., 2000; Færseth et al., 1995; Fossen et al., 2014; Gabrielsen et al., 1990; Gabrielsen et al., 2015; Klemperer, 1988; Klemperer and Hurich, 1990; Odinsen et al., 2000) those data rarely offer sufficient resolution for detailed structural configurations to be mapped with high confidence.

Deep reflection seismic data of good quality are available in the Egersund Basin area and have been utilized and studied with particular emphasis on the sub-salt (pre-Zechstein) sequences. The basement in the area likely carries the imprint of meso- to neo-Proterozoic mainly Fennoscandian orogeny (Bingen et al., 2005), Caledonian contraction and collapse (Bartholomew et al., 1993; Phillips et al., 2016; Reeve et al., 2014; Rey et al., 1997; Sørensen et al., 1992) and the effects of Variscan collision (Rey et al., 1997; Smit et al., 2016; Sørensen et al., 1992). In this context the WNW-ESE striking Tornquist system (e.g. Berthelsen, 1998; Pegrum, 1984) is a long-lived feature which was probably activated in connection with Caledonian contraction and reactivated in the Variscan and the Mesozoic (Pegrum, 1984; Phillips et al., 2018; Sørensen et al., 1992) and finally suffered tectonic inversion during the Alpine orogeny (Jackson et al., 2013; Mogensen and Jensen, 1994).

In the present work, 2D seismic lines of good quality were analyzed particularly to (i) establish the sediment distribution and structuring of the sub-salt sequences (which is not limited to the immediate sub-salt Rotliegend Group in this study) and the supra-salt structural framework of the larger Egersund Basin area (which includes the Egersund

* Corresponding author.
E-mail addresses: mohsen.kalani@gmail.com, kalani.m@nisoc.ir (M. Kalani).
[1] Present addressee: National Iranian South Oil Company (NISOC), Ahvaz 61,735–1333, Iran.

https://doi.org/10.1016/j.marpetgeo.2020.104642
Received 4 March 2019; Received in revised form 1 August 2020; Accepted 3 August 2020
Available online 6 August 2020

Basin, the Sele High, the Flekkefjord High, the Hummer Graben and the Farsund Basin; Fig. 1); (ii) identify and characterize supra-salt units; and (iii) investigate the possible role of the inherent sub-salt structural elements and depositional patterns and depocenters on the later post-/supra-salt basin development. The latter includes discussions on possible contributions of the Caledonian grain, and linkage of the Egersund Basin with the lithospheric-scale Sorgenfrei-Tornquist Zone.

2. Geological setting

The Egersund Basin is located to the east of the Central Graben in the Norwegian central North Sea. Its axis trends NW-SE as seen on the Late Jurassic-Early Cretaceous levels (e.g. Fjeldskaar et al., 1993; Irwin et al., 1993; Sørensen et al., 1992). It is bounded by the Stavanger Platform to the northeast, the Sele High to the northwest, the Flekkefjord High to the southwest and the Lista Fault Blocks to the southeast (Fig. 1b). The wider Egersund Basin area is underlain by E-W- and N–S trending rift structures reflecting at least two phases of Late Paleozoic extension. The precise timing of these events is, however, not well constrained. Tectonic lineaments with NE-SW-strike are situated closer to the Norwegian mainland. A large igneous province (LIP) centred on the Skagerrak area formed at about 300 Ma (Torsvik et al., 2008) and was followed by regional extension, crustal thinning and associated volcanism throughout the Permian-earliest Triassic (Heeremans and Faleide, 2004; Ziegler, 1990). According to Jackson and Lewis (2013, 2016) the eastern boundary fault system of the Egersund Basin (termed the Stavanger fault system in their work) was active during the late Permian and formed the northeastern margin of the North Permian Basin.

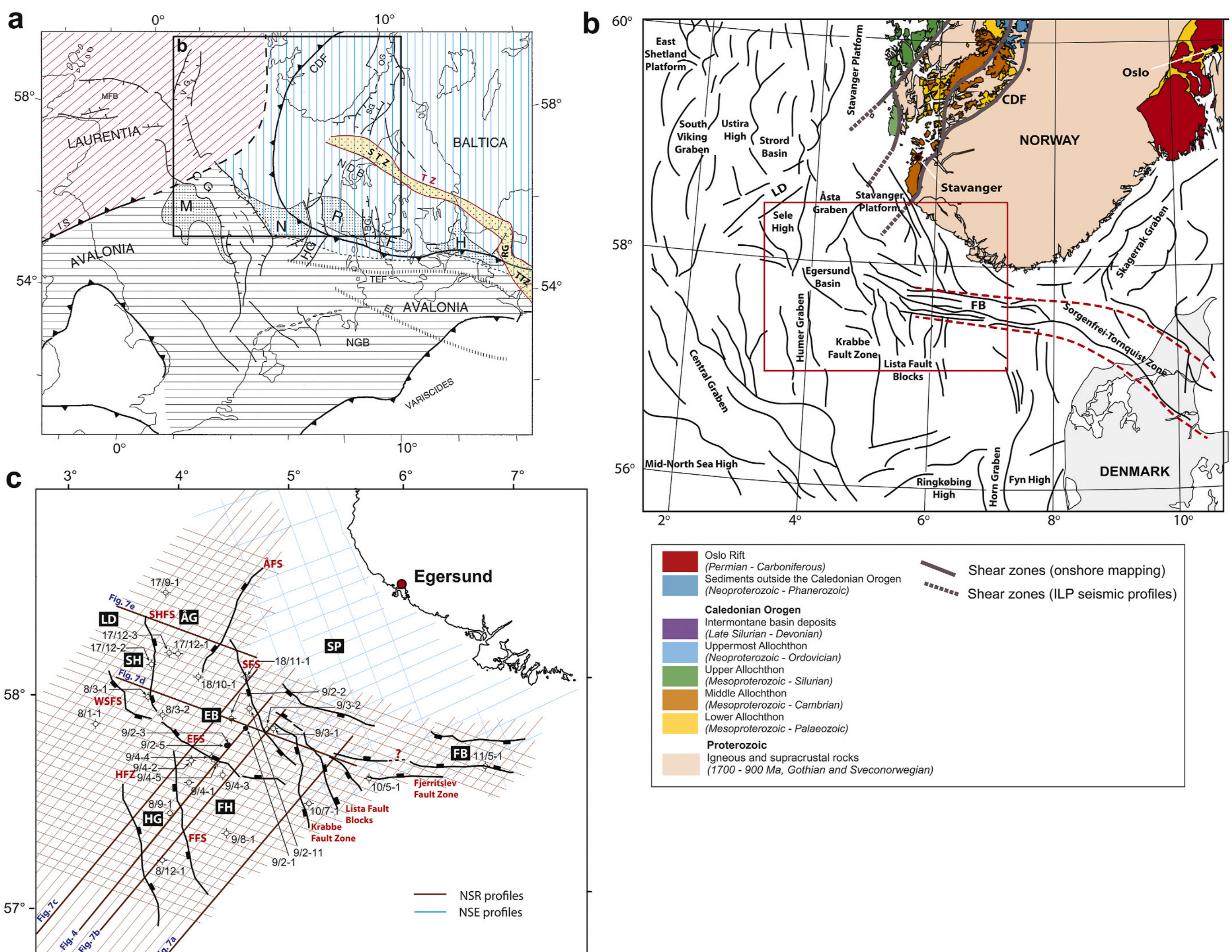

Fig. 1. (a) The North Sea area as the site of the triple plate collision of the Laurentia and Baltica continents and the East Avalonia microcontinent during the Caledonian Orogeny (slightly modified after Mona Lisa Working Group, 1997). Note the location of study area with respect to the Caledonian sutures and the continuation of the Sorgenfrei-Tornquist Zone. Abbreviations: BG – Brande Graben, CDF – Caledonian Deformation Front, CG – Central Graben, EL – Elbe Line, HG – Horn Graben, IS – Iapetus Suture, MFB – Moray Firth Basin, MNRFH – Mid North Sea–Ringkøbing–Fyn High, NDB – Norwegian–Danish Basin, NGB – North German Basin, OG – Oslo Graben, RG – Rønne Graben, SG – Skagerrak Graben, STZ – Sorgenfrei–Tornquist Zone, TEF – Trans European Fault Zone, TTZ – Teisseyre-Tornquist Zone. VG – Viking Graben; (b) Location and main structural features of the Central and Northern North Sea area. The study area is shown by the red box. Also, note the main onshore geological features of southern and western Norway. LD - Ling Depression, ÅG - Åsta Graben, SH - Sele High, SP - Stavanger Platform, EB - Egersund Basin, FH - Flekkefjord High, HG - Hummer Graben, FB - Farsund Basin, FT - Fjerritslev Trough, and CG - Central Graben; (c) Location of the utilized 2D seismic profiles and wells overlain by the master boundary fault systems interpreted at the Base Zechstein stratigraphic level. Selected profiles are highlighted and coded with numbers. Abbreviations: ÅFS - Åsta Fault system, EFS - Egersund fault system, FFS - Flekkefjord fault system, HFZ - Hummer Fault Zone, SFS - Stavanger fault system, SHFS - Sele High fault system, WSFS - West Sele fault system (Modified after Abramovitz and Thybo, 1999; Heeremans and Faleide, 2004; Phillips et al., 2016; Slagstad et al., 2011). (For interpretation of the references to color in this figure legend, the reader is referred to the Web version of this article.)

2.1. Plate tectonic setting

The North Sea area was the site of the triple plate collision of the Laurentia and Baltica continents and the East Avalonia microcontinent (Fig. 1a) during the mid Silurian–Early Devonian Scandian phase of the Caledonian Orogeny (Corfu et al., 2014; Roberts, 2003; Torsvik et al., 1997; Torsvik and Cocks, 2016). Before the eventual collision that affected the central and eastern North Sea area, the Tornquist Sea separated Baltica and East Avalonia whereas Laurentia was separated from the two opposing continents by the Iapetus Ocean. The accretion of Baltica and Avalonia along the Thor Suture (Pharaoh, 1999) most likely took place prior to the collision between Laurentia and Avalonia, as indicated by a convergence of palaeolatitudes as inferred from the onset of faunal mixing (Cocks and Fortey, 1982). During the Silurian a foreland basin developed in front of the Caledonian orogenic belt and major influx of clastic sediments from the uplifted mountain belt in the west filled the foreland basin throughout the Silurian and Early Devonian (Bruton et al., 2010).

The Baltica-Avalonia transition is represented by the Caledonian Deformation Front (CDF), which corresponds to a zone of thrusting at shallow level running along the southern flank of the Ringkøbing-Fyn High in offshore/onshore Denmark, and the Elbe-Odra Line at deep crustal level (Thybo, 2001). In such a picture, a wedge of Baltica crust extends from the Caledonian Deformation Front to the Elbe Line, representing remnants of the former passive margin of Baltica which was later overthrusted by East Avalonia (Maystrenko and Scheck-Wenderoth, 2013 and references therein). In the Early Devonian, Variscan collision began in the south which was responsible for east-west Caledonian divergence in Devonian times (e.g. Banka et al., 2002; Rey et al., 1997; Smit et al., 2016). Post-Caledonian extensional tectonics involved reactivation of low-angle thrusts and notably the basal décollement of the Caledonian thrust system, resulting in low-angle extensional shear zones (Mode I reactivation of Fossen, 1992) succeeded by formation of secondary large-scale extensional shear zones which transect the basal décollement and development of Devonian extensional basins (Mode II reactivation of Fossen, 1992). Such shear zones have been suggested to exist offshore southwest Norway (Fazlikhani et al., 2017; Fossen, 1992; Fossen et al., 2014, 2016; Fossen and Hurich, 2005) and also beneath the Egersund Basin (Phillips et al., 2016). Phillips et al. (2016) extrapolated low-angle shear zones farther to the south where (Abramovitz and Thybo, 1999, 2000) interpreted the CDF in the MONA LISA deep seismic profiles.

It is likely that the central and southern North Sea display contrasting late Caledonian and post-Caledonian developments, as suggested by different deep structural configurations. The weakness zones inherited from the Caledonian Orogeny and late syn-collisional to post-collisional stages along the Thor Suture involved strike-slip reactivations also along the Sorgenfrei-Tornquist Zone, and are believed to have been instrumental in the later development of the North Sea, including the Egersund Basin area, and southwest Scandinavia (Cherry, 1993; Gabrielsen et al., 2015; Harland, 1969; Lassen and Thybo, 2012; Pegrum, 1984; Phillips et al., 2018; Torsvik et al., 1997; Torsvik and Cocks, 2016).

3. Data and methods

3.1. Seismic reflection and well data

Parts of the long-offset 2D seismic survey North Sea Renaissance (NSR) acquired by TGS and Fugro Multiclient Services (2003–2012), were made available for this study. The maximum recording depth was 9.2 s (two-way time) with a good imaging quality down to 7–8 s, with a vertical resolution ranging between 10 and 20 m in the shallow subsurface to 40–50 m at depth, which offers seismic imaging beyond that seen in previous studies. The NSR survey provides a regional coverage in the North Sea area. It was acquired along NNE-SSW and ESE-WNW trending profiles in the central North Sea (Fig. 1c). The Stavanger Platform is covered by the 2D NSE-survey acquired by WesternGeco in the years 1980–1982 (Fig. 1c). The maximum recording depth is 6 s with a good imaging quality down to about 2 s, which is enough for reaching down to top acoustic basement. Some key technical and operational details of the surveys are listed in Table 1.

Wells located in quadrants 8–10 and 17 (Fig. 1c) were utilized to make the lithostratigraphic correlation scheme (Fig. 2, Table 2). Well data, including petrophysical logs and checkshots, were acquired from the Norwegian data repository for petroleum data (DISKOS). Selected well logs were utilized to facilitate the interpretation of selected seismic stratigraphic units, and to establish correlation schemes. These mainly include sonic transit time, bulk density, natural gamma-ray and neutron logs (Table 2). Stratigraphic tops and other relevant data including occurrences of metamorphic and igneous rocks were provided by the Norwegian Petroleum Directorate FactPages (http://www.npd.no/en/).

3.2. Seismic mapping

Selected seismic sequence boundaries (i.e. seismic horizons) and faults were manually traced in 2D seismic profiles by the use of IHS Kingdom® 2D PAK® interpretation tools. To facilitate seismic horizon picking, the attribute "PseudoRelief" implemented in the IHS Kingdom (IHS, 2013) was applied. The seismic horizons and corresponding sequences described below provided the basis for the present analysis. The primary focus was to establish a seismic and chronostratigraphic framework to interpret structural evolution, particularly to determine the fault history for the major basin boundary fault systems.

The obtained time-structure maps were utilized to calculate time-thickness (isochron) maps. The time-structure and isochron maps were

Table 1
Some major technical and operational details of the 2D seismic reflection surveys.

	Source	Streamer	Recorder
NSR-04 2004	Air gun: 3100–4258 in.^{3} Depth: 7 m Shot interval: 25 m	Group interval: 12.5–25 m Length: 8100 m Depth: 9 m	Record length: 9.2 s Sample rate: 2 ms Recording channels: 648 Nominal fold: 162
NSR-05 2004–2005	Air gun: 3100–5000 in.^{3} Depth: 7 m Shot interval: 25 m	Group interval: 12.5–25 m Length: 8100 m Depth: 7–9 m	Record length: 9.2 s Sample rate: 2 ms Recording channels: 648\324 Nominal fold: 162
NSR-06 2006	Air gun: 3410–5000 in.^{3} Depth: 7m Shot interval: 25 m	Group interval: 12.5 m Length: 8100 m Depth: 9 m	Record length: 9.2 s Sample rate: 2 ms Recording channels: 648\ 640 Nominal fold: 162\ 160
NSE 1980–1982	Shot interval: 25 m	Group interval: 25 m ?	Record length: 6 s Sample rate: 4 ms

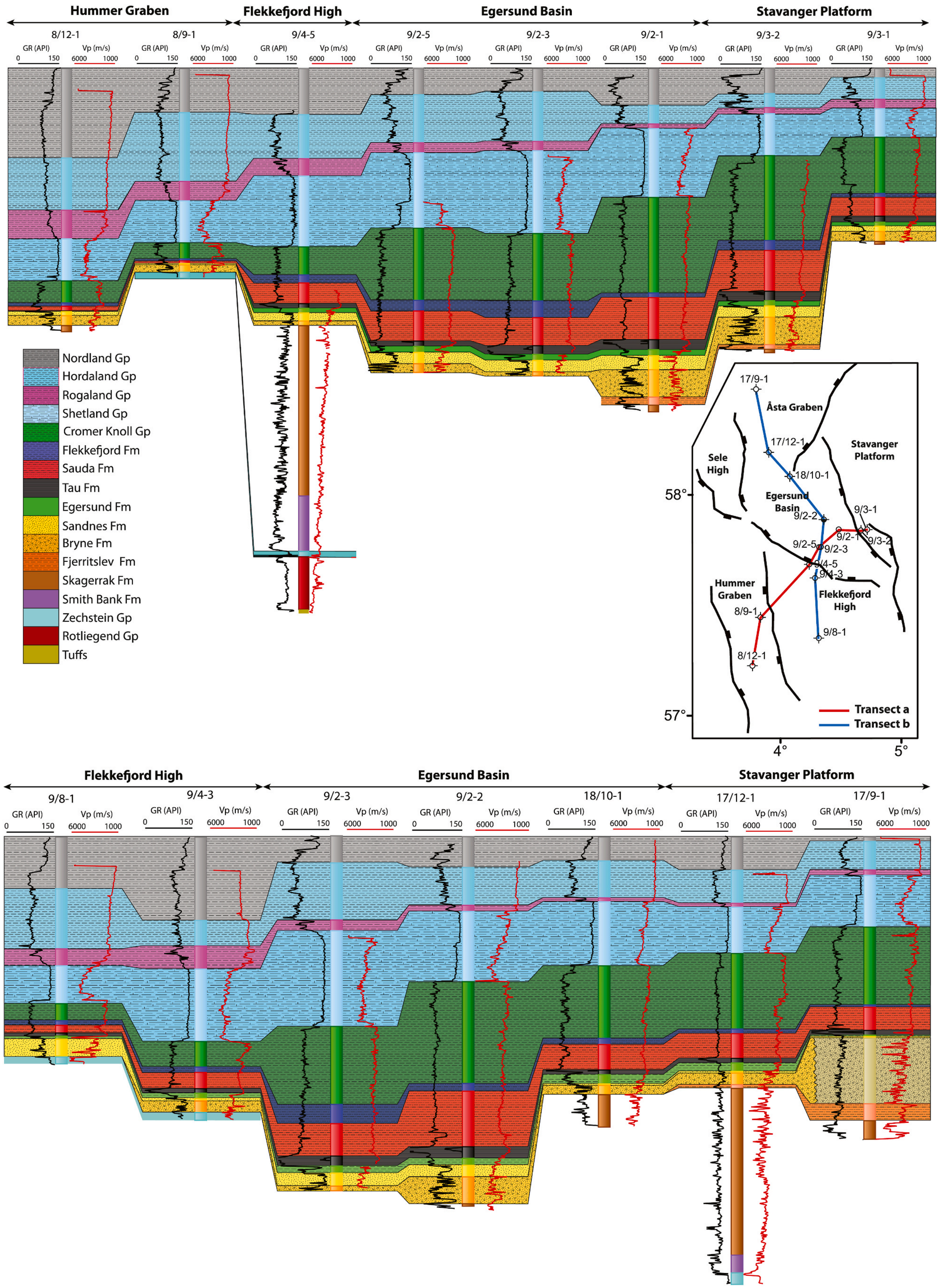

Fig. 2. Lithostratigraphic correlation through the exploration wells across the study area. Note the location of boreholes and the structural elements each of the wells passes over. More detailed lithostratigraphy can be found in Fig. 3.

Table 2
Well log data availability to this study.

Well list	GR	RHOB	DT	NPHI	RES	T-D
8/1-1	✓	×	✓	×	✓	×
8/3-1	✓	×	✓	✓	✓	×
8/3-2	✓	✓	✓	✓	✓	×
8/9-1	✓	✓	✓	✓	✓	✓
8/12-1	✓	✓	✓	✓	✓	✓
9/8-1	✓	✓	✓	×	✓	✓
9/2-1	✓	✓	✓	✓	✓	✓
9/2-2	✓	✓	✓	✓	✓	✓
9/2-3	✓	✓	✓	✓	✓	✓
9/2-4s	✓	✓	×	✓	✓	✓
9/2-5	✓	✓	×	✓	✓	×
9/2-6s	✓	✓	✓	✓	✓	×
9/2-7s	✓	✓	✓	✓	✓	×
9/2-8s	✓	✓	×	✓	✓	✓
9/2-9s	✓	✓	×	✓	✓	×
9/2-11	✓	✓	✓	✓	✓	✓
9/3-1	✓	✓	✓	✓	✓	✓
9/3-2	✓	✓	✓	✓	✓	✓
9/4-1	✓	✓	✓	×	✓	×
9/4-2	✓	×	✓	×	✓	×
9/4-3	✓	✓	✓	×	✓	✓
9/4-4	✓	✓	✓	✓	✓	✓
9/4-5	✓	✓	✓	✓	✓	✓
10/5-1	✓	✓	✓	✓	✓	✓
10/7-1	✓	✓	✓	✓	✓	✓
10/8-1	✓	✓	✓	×	✓	✓
17/9-1	✓	✓	✓	✓	✓	×
17/12-1R	✓	✓	✓	×	✓	✓
17/12-2	✓	✓	✓	✓	✓	✓
17/12-3	✓	✓	✓	✓	✓	✓
18/10-1	✓	✓	✓	✓	✓	✓
18/11-1	✓	✓	✓	×	✓	✓

used to investigate structural elements and their temporal evolution.

Structural nomenclature was adapted from the Norwegian Petroleum Directorate Fact Map (http://www.npd.no/en/) or other published literature where applicable. In the absence of published formal or informal names, new nomenclature has been assigned according to the principles suggested by Gabrielsen et al. (1984) and Nystuen (1989). In this paper, informal nomenclatures were printed entirely in lower case whereas formal names have been capitalized.

Potential igneous features were inferred based on the geometry and likely lithology variations, the external form and the internal reflection configurations (cf. Magee et al., 2013; Planke et al., 2000, 2005). Alternative interpretations of strong dipping reflections at depth were also considered.

4. Seismic stratigraphic framework

Six seismic horizons, bounding five seismic sequences (the Rotliegend Group and the sub-Rotliegend sequences I-IV; Figs. 3 and 4), were mapped below the upper Permian Zechstein salt, particularly emphasising the establishment of the sub-salt structural configuration. Except for the Rotliegend Group, there is limited well control for the interpreted seismic sequences below the salt. Sub-salt well data are limited to a few wells located on structural highs relatively far away from the main area of interest. Hence, the sub-Rotliegend sequence boundaries 1–4 (SRSB 1–4) were mainly identified based on reflection character and terminations only.

For the Rotliegend Group and its overlying sequences, which have been penetrated by several wells, selected lithostratigraphic levels (the Base Zechstein, the Mid-Jurassic unconformity, the Top Tau Formation, the Top Sauda Formation, the Top Cromer Knoll Group and the Top Shetland Group) were tied to the seismic data and utilized in the mapping (Figs. 3 and 4). Well log and seismic expression of the stratigraphic units are illustrated and summerized in Figs. 2 and 5, respectively. The stratigraphic units and corresponding seismic sequences are described in more detail below (chapter 6).

5. Structural interpretations and evolution of the fault systems

Because the sub-salt and supra-salt structural configurations display significant differences, time-structure maps of these structural levels as well as the base Zechstein Group are presented (Fig. 6a–c).

5.1. Selected time-structure maps

5.1.1. The sub-rotliegend sequence boundary 4 (top acoustic basement)

Amoung the sub-salt sequence boundaries the SRSB 4 is the deepest one which shows notable syn-tectonic related time-depth variations. SRSB 4 is the deepest sequence boundary that can be mapped throughout the study area and is taken to represent the top of the acoustic basement (e.g. Fig. 4). The SRSB 4 level is strongly faulted, displaying a pronounced, composite relief and an overall dip of the top basement surface towards the SW. Four major fault populations (N–S, E-W, NE-SW, and NW-SE) are distinguishable, the N–S and E-W trends are dominating while the NW-SE and NE-SW trends are less well pronounced (Fig. 6a). These four major fault trends define the main structural elements of the greater Egersund Basin area (cf. Figs. 1c and 6a).

5.1.2. Base of the Zechstein Group

The Base-Zechstein Group provides a regionally well mappable (i.e. acoustically shows a high contrast) expression of the Late Paleozoic in the larger Norwegina-Danish Basin. The time-structure map at the base of the Zechstein Group (Fig. 6b) displays a wider area of subsidence and major normal fault populations that only partly correlate with the deeper structures. These faults displace the SRSB 1 level as well as the base of the Rotliegend Group and the base of the Zechstein Group. A distinct contrast in structural configuration is still identified at the base of the Zechstein Group (cf. Fig. 6 b) as compared to that of the SRSB 4 level (Fig. 6a) in that the prominent E-W basin configuration is constrained to the levels below the SRSB 2.

5.1.3. The mid-Jurassic Unconformity

The mid-Jurassic Unconformity is a regionally mappable unconformity associated with magmatism during early rift development in the central North Sea (Underhill and Partington, 1993). The time-structure map of the mid-Jurassic level (Fig. 6c) clearly displays the NW-SE trend of the Egersund Basin proper and the deepening in the hangingwalls of some of the N–S trending faults (e.g., in the Åsta Graben).

5.1.4. Top Cromer Knoll Group

The top of the Cromer Knoll Group overlain by chalks and therefore acoustically showing a high contrast, represents an important change of the supra-salt basin configuration is presented (Fig. 6d), displaying folds related to tectonic inversion. Top Cromer Knoll Group is dominated by NW-SE-faults (Fig. 6d) and shows a general pattern of deepening towards the Central Graben in the southwest. The time-structure map also displays a number of asymmetrical folds in the fault hanging walls related to tectonic inversion. This is particularly the case for the Stavanger fault system northeast of the Egersund Basin.

5.2. Main structural elements

Selected seismic profiles crossing the main structural elements are shown in Fig. 7. The most important structural elements within the study area are the following:

The *Egersund Basin* is separated from the Stavanger Platform in the northeast by a NNW-SSE trending fault system informally termed the Stavanger fault system (SFS) by Jackson and Lewis (2013) and Lewis et al. (2013) (Figs. 1c, 4 and 6a and 7b-d). The NW-SE trending faults, which separate the Egersund Basin from the Flekkefjord High to the south, are labelled the Egersund fault system (EFS) here. In the east, the

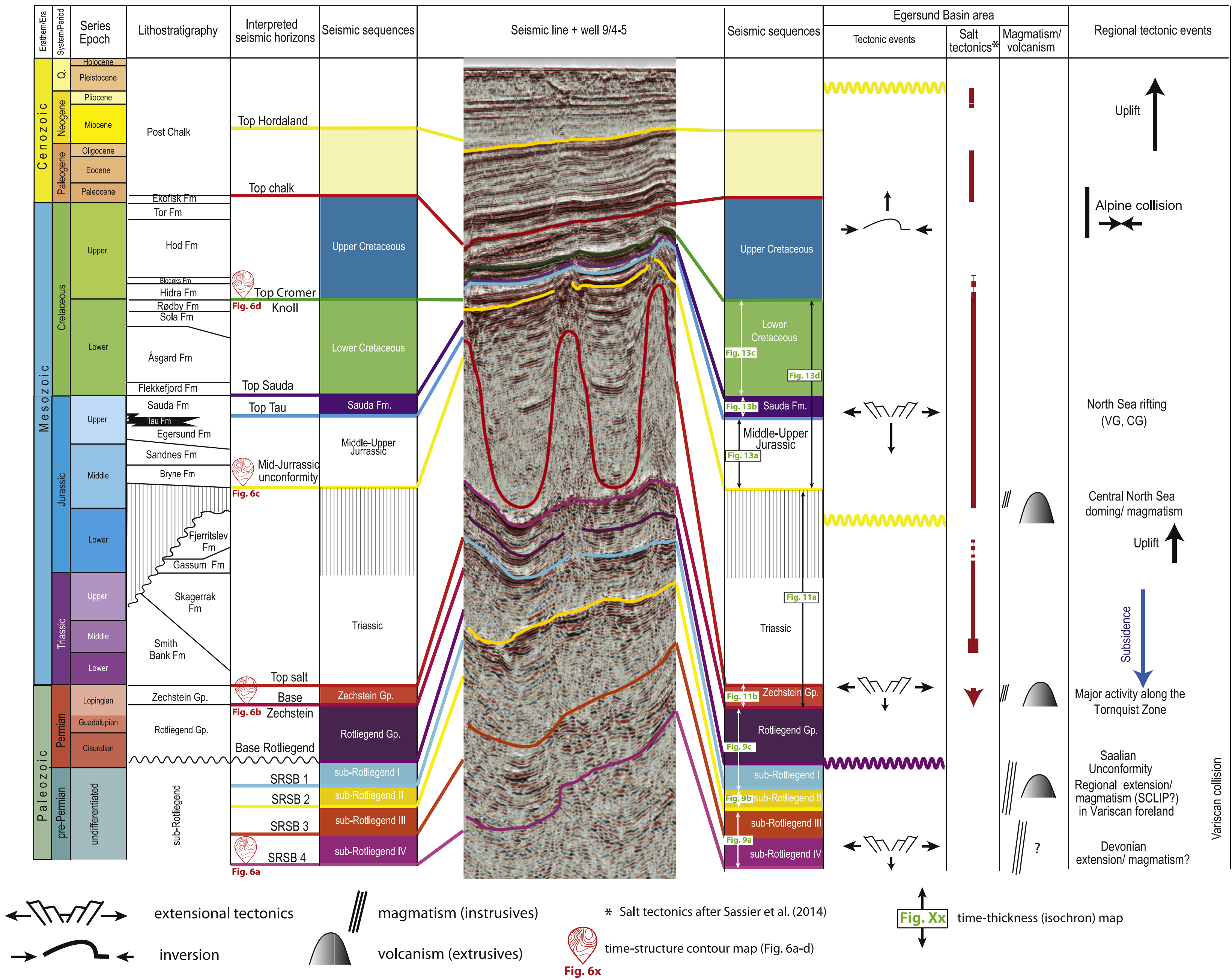

Fig. 3. Lithostratigraphy, interpreted seismic horizons and corresponding sequences, and main regional and local tectonic events.

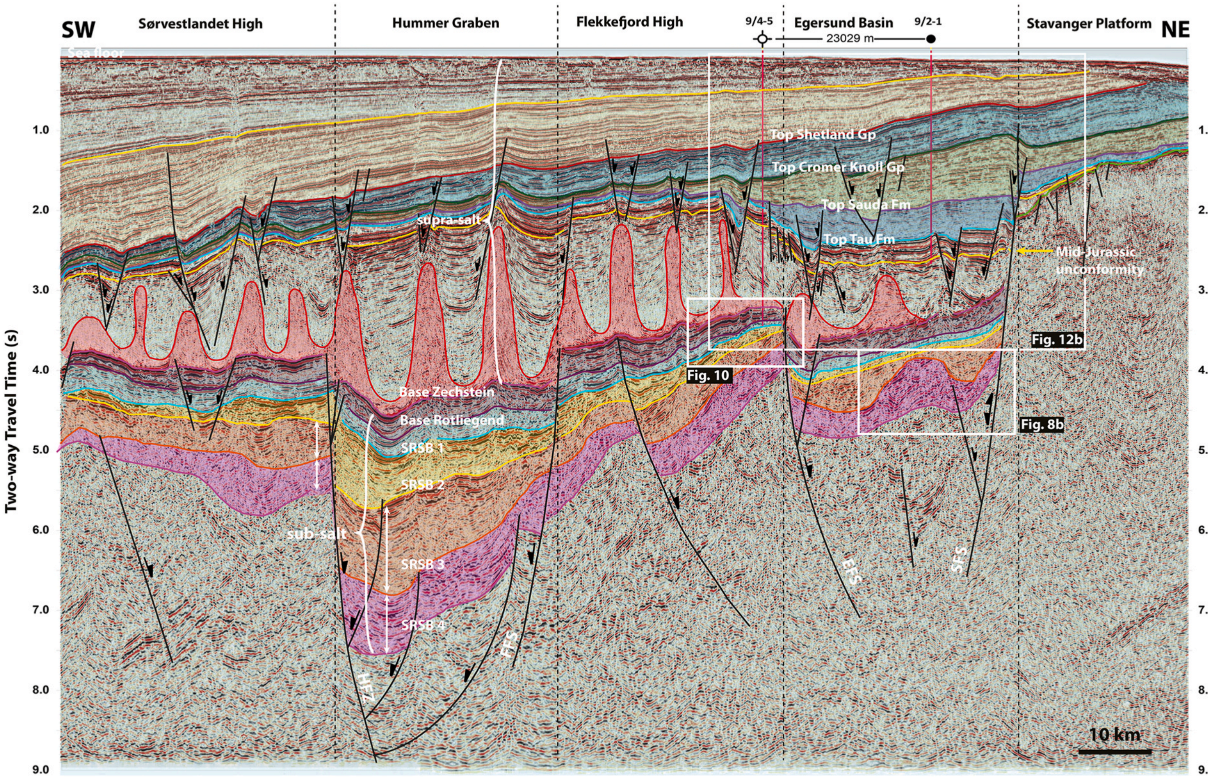

Fig. 4. Selected seismic profile showing main interpreted depositional and structural features. Abbreviations: ÅFS - Åsta Fault system, EFS - Egersund fault system, FFS - Flekkefjord fault system, HFZ - Hummer Fault Zone, SFS - Stavanger fault system, SHFS - Sele High fault system, WSFS - West Sele fault system. For the colors assigned to the seismic sequence boundaries and sequences see Fig. 3. Data courtesy of TGS. (For interpretation of the references to color in this figure , the reader is referred to the Web version of this article.)

Egersund Basin is bounded by the northern segment of the N–S striking Krabbe Fault Zone (Figs. 1c, 6a and 7d).

The *Åsta Graben* forms a northward continuation of the Egersund Basin between the Sele High and the Stavanger Platform (Figs. 1b, 6b and 7a). It is separated from the Sele High in the west by the N–S striking Sele High fault system (SHFS), and from the Stavanger Platform in the east by the NE trending Åsta fault system (ÅFS) (Fig. 7e).

The continuation of the Egersund fault system towards the Sele High, which separates the Sele High from the larger Norwegian-Danish Basin, is named the West Sele fault system (WSFS) in the present work (Fig. 1c).

The *Hummer Graben*, which is characterized by a N–S-striking graben axis is separated from the Flekkefjord High on its east by the Flekkefjord fault system (FFS), which consists of planar normal faults (Figs. 4 and 7b,c). The fault zone that separates the Hummer Graben from the Sørvestlandet High on its west is termed the Hummer Fault Zone (Norwegian Petroleum Directorate FactMaps). The Hummer Graben widens from the south to the north at the SRSB 4 stratigraphic level (Fig. 6a), being part of a larger structural low. The dominant N–S striking structures associated with the Hummer Graben cut E-W striking normal planar faults bounding the prominent E-W trending Ytterbanken graben (Figs. 6a and 7a-c). The most prominent faults associated with this E-W basin structure are the Southern Flekkefjord High border fault and the Northern Sørvestlandet High border fault. These normal faults have throws to the south and north respectively. The SRSB 4 is at its deepest in the centre of the Hummer Graben where the N–S trending fault systems cross-cut the E-W trending fault systems (Fig. 6a).

6. Basin configurations and sedimentary infill

6.1. Intra-basement reflections

A tilted seismic unit, which is characterized by high-amplidude parallel to sub-parallel seismic reflections has been identified locally beneath the interpreted top acoustic basement horizon (Figs. 4 and 7). This unit is suggested to include Devonian shear zones by Phillips et al. (2016) and Fazlikhani et al. (2017) beneath the Egersund Basin and in the larger northern North Sea area as well. According to Fazlikhani et al. (2017) the intra-basement medium-amplitude seismic facies unit probably represents less sheared crystalline basement of Proterozoic or Paleozoic (Caledonian) origin compared to the Devonian shear zones.

No well has reached basement in the central part of the Egersund Basin, preventing further lithologic characterization of the basement here. For the same reason, the lower boundary of the sequence can not be constrained with certainty. However, a few wells in the greater Egersund Basin area shed some light on the lithological nature of this part of the acoustic basement. Well 8/3-1 situated at the eastern flank of the Sele High (Fig. 1c) was terminated in metamorphic rocks (schists) having a K/Ar radiometric age of earliest Devonian (411 $\pm$ 4 Ma; Myhre, 1975). Well 17/12–2, also at the Sele High (Fig. 1c) was terminated in a sandstone of likely Devonian age (http://factpages.npd.no). Thus, a general Devonian age can be assigned to the stratified unit observed locally at the top of the acoustic basement in the study area. Well 11/5–1, which is located farther east on the southern flank of the Farsund Basin (Fig. 1b) reached a meta-sedimentary basement of Silurian age, more representative of the foreland to the Caledonides.

6.2. Sub-Rotliegend sequences IV and III

The sub-Rotliegend sequence IV is bounded by the SRSB 4 at its base and SRSB 3 at its top. SRSB 3 marks an erosional unconformity and is cut by the same fault systems that affects SRSB 4 (see “main structural elements” section above). SRSB 2, at the top of sub-Rotliegend sequence III is also associated with erosional truncation and is gently inclined (Fig. 4).

Seismic reflection characteristics	Interpretation	Occurrence	Examples *
Channel-levee seismic facies unit sandwiched by lower and upper moderate to high amplitude and high continuity seismic facies	deltaic and shallow marine seiments with distributary channels developed in between	Pliocene- Quaternary upper Hordaland and Nordland Gp	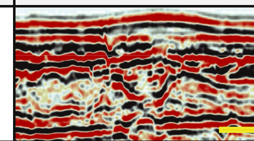
High continuity and variable but generally low amplitude parallel to divergent reflections	Marine fine-grained dominated clastic sediments	Eocene-Miocene Hordaland Gp	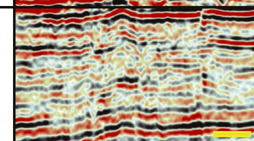
High continuity and variable amplitude parallel to divergent reflections	Alternation of fine and coarse-grained clastic sediments	Paleocene- Eocene Rogaland Gp	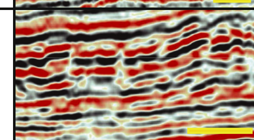
High continuity and variable but generally high amplitude parallel reflections	Chalk	Upper Cretaceous Shetland Gp	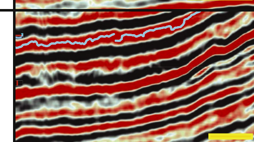
Three seismic facies units consisting of slightly divergent to parallel reflections. The middle high continuity and high amplitude one under- and overlain by lower high continuity and low amplitude and upper moderate continuity, high amplitude and low frequency facies units	Deep marine sediments sharply transiting into chalks. Within the chalk increasing argillaceous sediments caused to decreased amplitudes	Lower- Upper Cretaceous Cromer Knoll and Shetland Gp	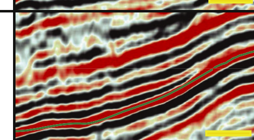
Sigmoidal seismic facies unit sandwiched by lower relatively low amplitude and moderate continuity sub-parallel seismic facies and upper moderate to high amplitude and high continuiy seismic facies	prograding sediments close to continental shelf edge	Upper Jurassic-Lower Cretaceous Sauda and Flekkefjord Fm	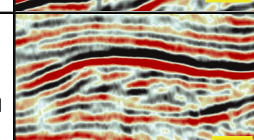
Lower facies unit consisting of alteration of high continuity parallel reflections with variable but increasing upward amplitudes is overlain by upper high continuity and low amplitude sub-parallel seismic facies unit	Lower coarse-grained dominated deltaic to shallow marine facies overlain by fine-grained dominated deep marine facies	Middle-lower Upper Jurassic Bryne, Sandnes, Egersund and Tau Fm	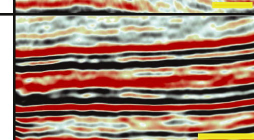
Wedge formed seismic facies units with internal high amplitude, moderate continuity and relatively high frequency divergent reflection configurations, terminating towards chaotic reflections on both sides	clastic sediments accommodated in between salt intrusions (salt walls)	Triassic	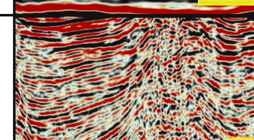
Sub-parallel and chaotic low amplitude to reflection free seismic facies	Salt walls and clastic sediments (possibly slumped) accommodated in between	Upper Permian (Zechstein Group) and Triassic	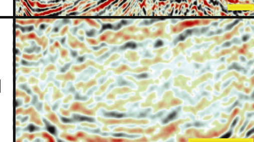
Dominantly high continuity, high amplitudes and relatively low frequency parallel/sub-parallel to divergent with local chaotic to reflection free seismic facies found as sheets and sheet drapes	Clastic dominated marine to fluvial (coarsening upward) sediments with locally distributed volcanoclastics	Sub- Rotliegend II, I and the Rotliegend Group	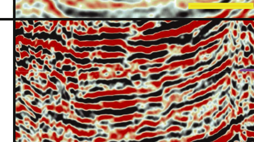
High amplitude reflections associated sub-parallel low amplitude with moderate continuity	potential intrusions or shear zone related reflections	Sub- Rotliegend IV & III	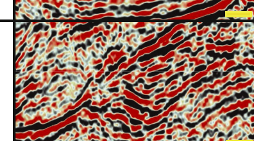
Parallel/sub-parallel to steeply divergent and high amplitude associated with chaotic facies	Clastic dominated sediments locally distorted due to deep burial and tilting or shear zone related reflections	Sub- Rotliegend IV & III	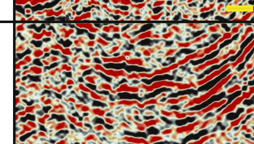

* Vertical scale: 0.1 s (TWT), Horizontal scale: 1 km

Fig. 5. Summary of seismic expression of the studied seismic stratigraphic units.

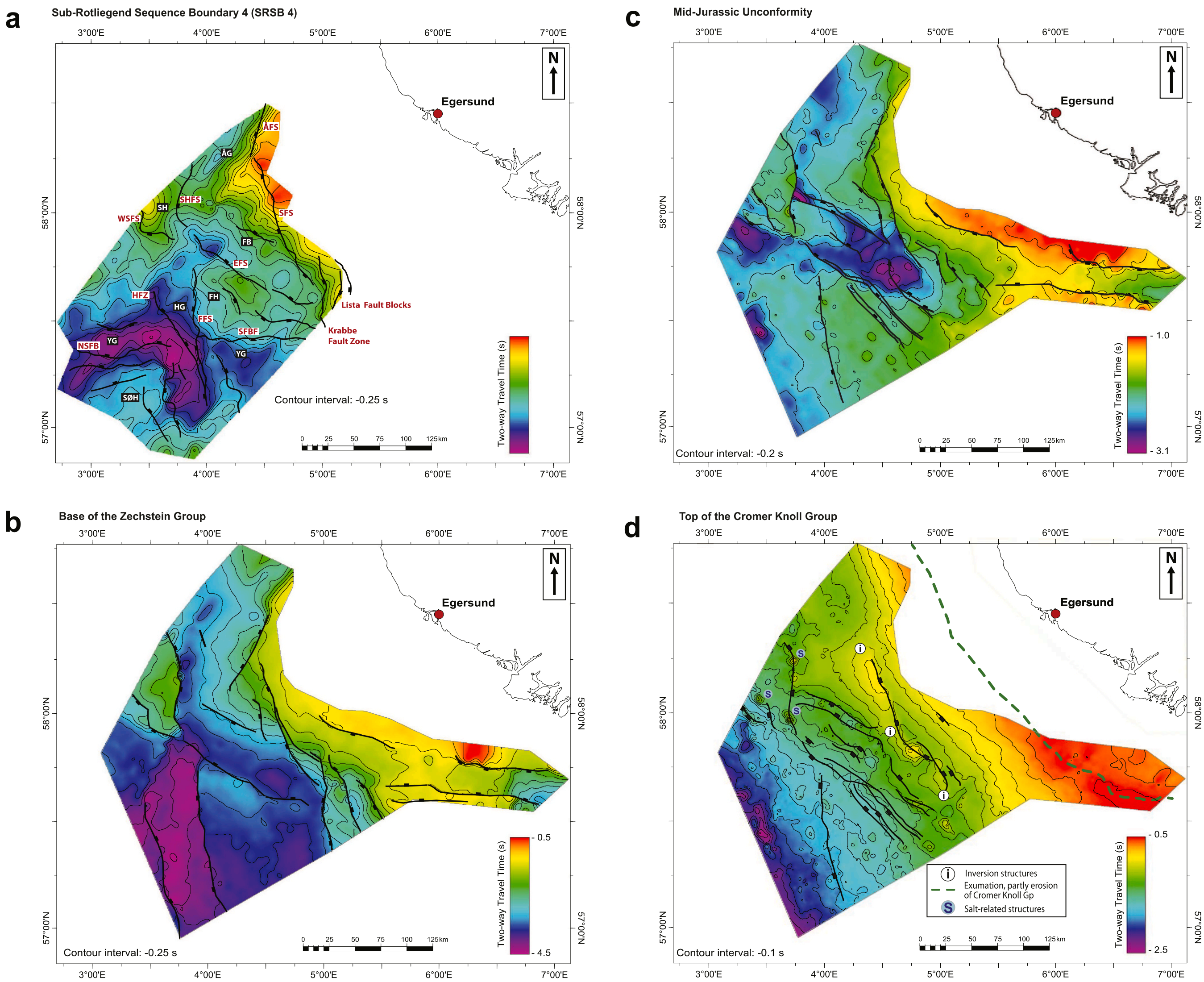

Fig. 6. (a) Time-structure map at the SRSB 4 (top acoustic basement) showing the deep basin configuration; (b) Time-structure map at the base of the Zechstein Group. Depth variation and normal fault trends are consistent and show prominent change compared to structural impacts at the SRSB 2 and its underlying sequence boundaries; (c) Time-structure map at the Mid-Jurassic unconformity; (d) Time-structure map at the top Cromer Knoll Group. Note inversion along the northern flank of the Egersund Basin and the eastern flank of the Åsta Graben labelled with circled "i" and salt related structures labelled with circled "S". Abbreviations in black blocks refer to structural elements: ÅFS- Åsta fault set, ÅG- Åsta Graben, EB- Egersund Basin, EFS- Egersund fault system, Fault abbreviations are printed in red: FFS- Flekkefjord fault system, FH- Flekkefjord High, HFS- Hummer Fault Zone, HG- Hummer Graben, NSBF- Northern Sørvestlandet High border fault, SFBF- Southern Flekkefjord High border fault, SFS- Stavanger fault system, SH- Sele High, SHFS- Sele High fault system, SØH- Sørvestlandet HighSP- Stavanger Platform, WSFS- West Sele fault system, YBG- Yetterbanken graben. (For interpretation of the references to color in this figure, the reader is referred to the Web version of this article.)

These sequences partly include and partly are bounded by steeply inclined high-amplitude reflections with moderate to low continuity which are associated with less inclined and internally folded reflections. This characteristic seismic facies unit has previously been interpreted as shear zones (Phillips et al., 2016). According to Phillips et al. (2016), the deepest and most shallowly dipping intra-basement reflections of package IP1 are associated with more steeply dipping seismic reflection packages (IP2-IP4; Phillips et al., 2016) and individual Caledonian thrusts and shear zones onshore South Norway (Fossen, 2010 and references therein). They can also be correlated to reflections in deep seismic profiles ILP (Fossen et al., 2014; Gabrielsen et al., 2015) and MONA LISA (Abramovitz and Thybo, 1999, 2000) located to the northeast and south of the Egersund Basin, respectively.

In some places, observations of high amplitude reflections cross-cutting the layering of the sub- Rotliegend IV and III offer an alternative interpretation as potential igneous rocks, intruding the sub-Rotliegend sequences III and IV (Fig. 8). With regard to the geometry of the mentioned seismic facies, the main potential intrusive features are both dykes and sills. The steeply inclined reflections are particularly observed on the NW-SE trending seismic profiles (e.g. Figs. 7d and 8b) and are geometrically comparable to seismic signatures interpreted as dykes in the Farsund Basin by Phillips et al. (2017) whereas less inclined partly internally folded reflections are comparable with those interpreted as sills (e.g. Hansen and Cartwright, 2006; Planke et al., 2005; Rocchi et al., 2007). The reflections interpreted to be sills display patterns ranging from layer-parallel straight and folded ones to concave-shaped structures believed to represent sill complexes (Fig. 8b and c). See chapter 6.4 for age discussion of the potential intrusives.

Extrapolation of the shear zone related to the CDF (i.e. basal decollemant of the Caledonian thrust belt; IP1 of Phillips et al., 2016) towards the south (MONA LISA seismic profiles 1–4), however, allows to adapt the interpretation of Lyngsie and Thybo (2007) of the MONA LISA

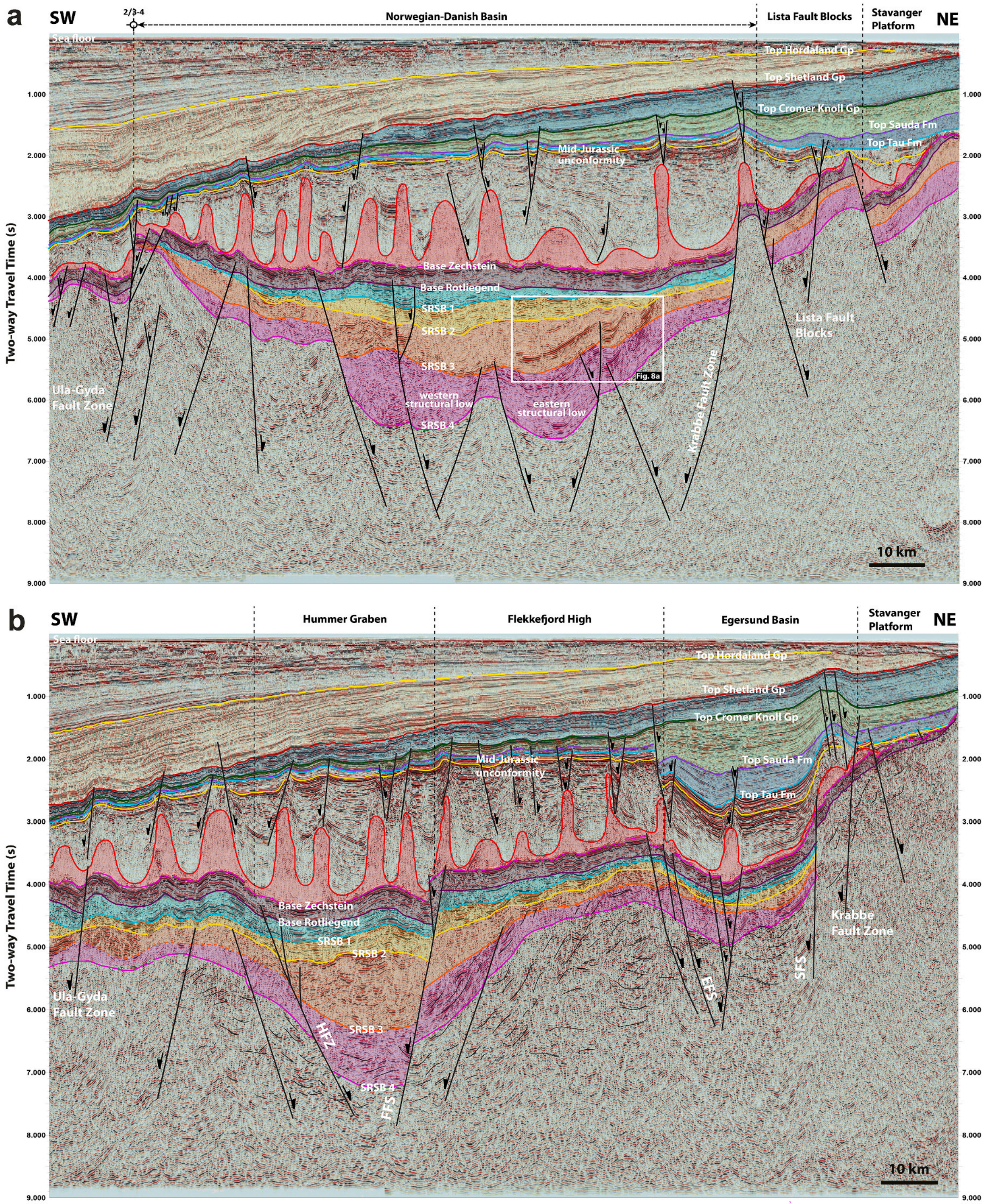

Fig. 7. Selected seismic profiles showing main interpreted depositional and structural features in different parts of the study area. Abbreviations: SFS - Stavanger fault system, ÅFS - Åsta fault set, EFS - Egersund fault system, SHFS - Sele High fault system, FFS - Flekkefjord fault system, HFZ - Hummer Fault Zone. For location of the seismic profiles, see Fig. 1c. For the colors assigned to the seismic sequence boundaries and sequences see Fig. 3. a) SW-NE trending seismic line representing larger Norwegian-Danish Basin bordered by the Krabbe and Ula-Gyda fault zones, in the east and west, respectively. The sub-salt eastern and western structural lows are the southern continuation of the Hummer Graben and the eastern extension of the Ytterbanken graben, respectively. b) SW-NE trending seismic line passing through Hummer Graben, Flekkefjord High and Egersund Basin. Note that the Flekkefjord High is rather wide while the Hummer Graben comprises relatively narrow structural low. Features beneath the interpreted top acoustic basement are potentially related to Devonian shear zones as identified onshore and discussed in Phillips et al. (2016) and Fazlikhani et al. (2017). c) SW-NE trending seismic line passing through the Ytterbanken graben, Hummer Graben, Flekkefjord High and Egersund Basin. The E-W trending Ytterbanken graben is the most conspicuous structural feature at the sub-salt level. d) NW-SE seismic line passing through the Sele High, Egersund Basin and Lista Fault Blocks. e) NW-SE seismic line passing through the Sele High, Åsta Graben and Stavanger Platform. Note the uniform thickness of the lower Triassic unit and thickening of middle and upper Triassic units suggesting that salt withdrawal related folding initiated during the Middle Triassic and continued in the Late Triassic though the Jurassic. Data courtesy of TGS. . (For interpretation of the references to color in this figure, the reader is referred to the Web version of this article.)

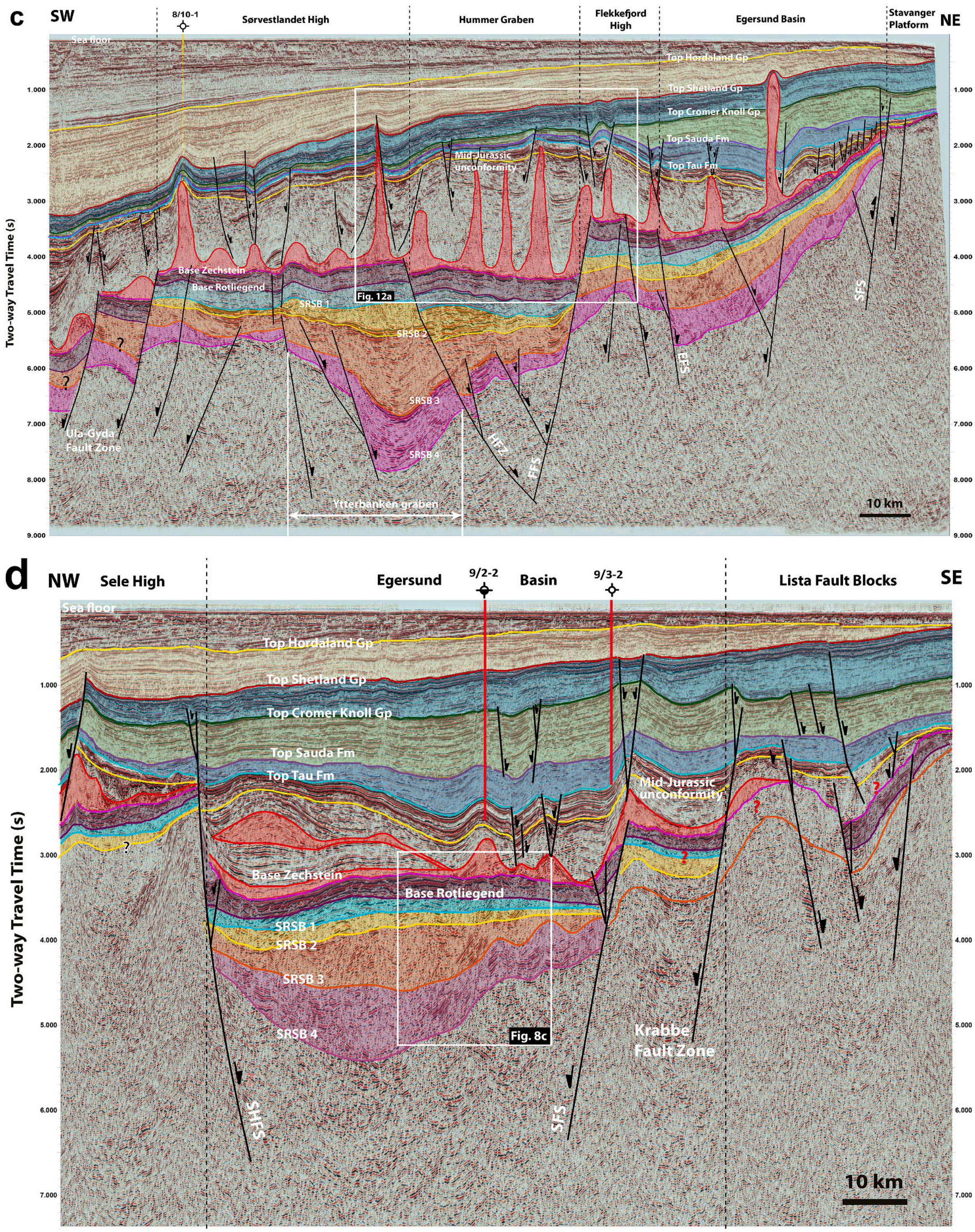

Fig. 7. (*continued*).

profile 3. Based on the gravity and magnetic modelling, Lyngsie and Thybo (2007) argued that brittle reactivation of pre-existing shear zones or thrust planes were utilized by the intrusives in relation with the late Paleozoic extension of the lithosphere (i.e. Carboniferous-Permian rifting). Such an interpretation of the of the MONA LISA profile 3 is further supported by the widespred intrusive and extrusive magmatism along the East North Sea High and the Ringkøbing-Fyn High, associated with the Variscan orogenic compression and the imposed crustal thining and extension by the end of the Carboniferous (Dixon et al., 1981).

Beneath the central and southern parts of the N–S trending Hummer Graben and the E-W trending Ytterbanken graben sub-Rotliegend sequences IV and III are characterized by slightly divergent reflections onlapping the SRSB 4 and SRSB 3 within several distinct depocenters (sub-basin centers; Figs. 4 and 6a,b). These depocenters are commonly aligned. The maximum sediment thickness is 2.4 s where these two trends cross-cut (Fig. 9a). While the depocenters are largely considered of similar age, with respect to the deepest E-W trending structures/depocenters as inferred from the sub-Rotliegend sequences III and IV isochron values and the cross-cutting relationship, they are inferred to have developed prior to the N–S trending structures/depocenters by the

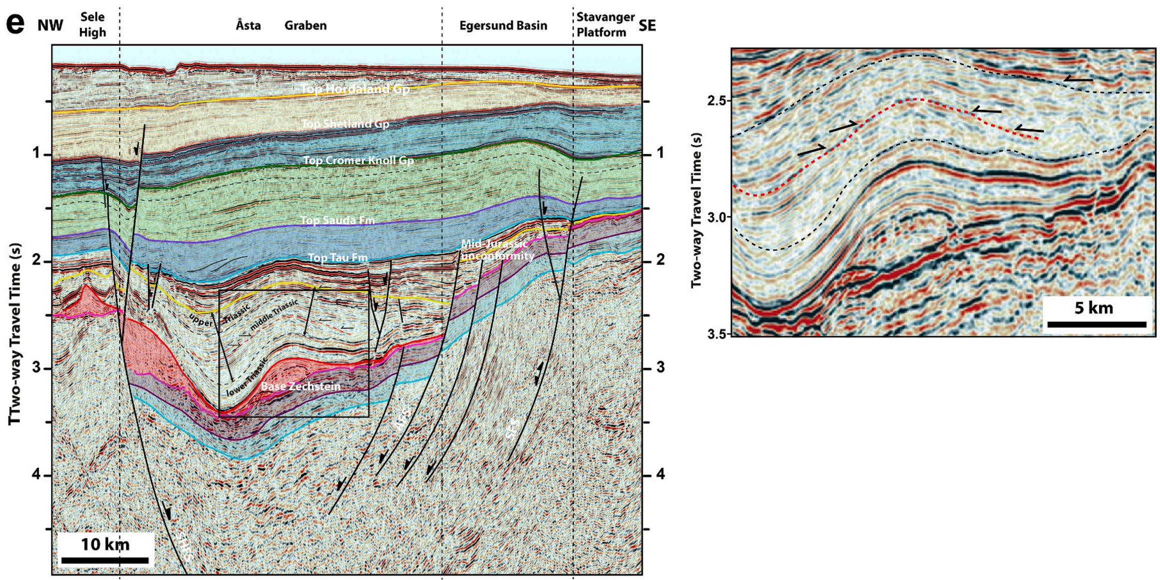

Fig. 7. (*continued*).

Late Devonian.

The NE-SW and NW-SE structural trends (Fig. 1c) had minor effect on developments of the depocenters during deposition of the sub-Rotliegend sequence IV and III. The expansion of the sequence in the hanging walls of the main faults and the tilt of the sedimentary units suggest syn-tectonic deposition for the sub-Rotliegend sequences IV and III with both E-W and N–S trends.

6.3. Sub-Rotliegend sequence II

The lower boundary of the sequence (SRSB 2) is characterized by a gently inclined (basin-center-directed) reflector with no or minor growth at hangingwall of the major boundary faults (e.g minor growth in hangingwall of HFZ) and reflections onlapping basin margins, whereas the top, SRSB 1, is largely parallel with the overlying sub-salt reflections.

The isochron map of the sub-Rotliegend sequence II (Fig. 9b) reflects thickening in areas which coincide with the major depocenters of the underlying sequences with a maximum isochron value of 0.9 s beneath the Hummer Graben and in the immediate hanging wall of the Egersund fault system (Fig. 9b). The coincidence of minor thickness variations and burial of some of the main pre-existing normal faults likely reflect post-extensional deposition, and differential compaction of the underlying basin units.

6.4. Sub-Rotliegend sequence I and Rotliegend Group

The sub-Rotliegend sequence I and the Rotliegend Group are separated from each other by the Saalian Unconformity (NPD, 2016). At the Flekkefjord High this unconformity forms an erosional truncation. In deeper settings, the Saalian Unconformity is developed as a disconformity (Fig. 4). The base of the Rotliegend Group (i.e. Saalian Unconformity) is mostly parallel to the base of the Zechstein Group.

Locally, the sub-Rotliegend sequence I contains more chaotic and mounded facies. On the Flekkefjord High, a chaotic reflection bundle within the sub-Rotliegend sequence I was tied to the tuffs in which well 9/4–5 terminated (Fig. 10). The Rotliegend Group in well 9/4–5 comprises a lower shale unit overlain by a thick conglomerate-dominated unit, which again is overlain by alternating sandstones and mudstones (Fig. 10). The sub-Rotliegend sequence I and its underlying sequences are cut by bundels of reflections which are comparable to the typical seismic signature of intrusives (e.g. Hansen and Cartwright, 2006; Planke et al., 2005; Rocchi et al., 2007). Accepting a dyke interpretation for the steeply inclined reflections (either they have used existing fracture networks of the Devonian Shear zone or not), with respect to the thinning of the Rotligend Group just above, these are interpreted as mostly reaching up to the base of the Rotliegend Group (i.e. Saalian Unconformity). Thus, the probable dykes and the associated sill complexes (e.g. Fig. 8) are inferred to be emplaced close to the Carboniferous-Permian transition (i.e. 296-300 Ma). This is in agreement with the dyke swarm recently reported from the adjacent Farsund Basin (Phillips et al., 2017).

The isochron map of the combined sub-Rotliegend sequence I and Rotliegend Group (Fig. 9c) indicates gentle subsidence along NE-SW oriented axes, which can be correlated to the deeper basin configurations as described above to a limited degree only (Fig. 6a–d). The rather uniform thickness of the sub-Rotliegend sequence I and Rotliegend Group across major faults suggests that the pre-existing faults were dormant during this time period, and that the prominent faults at the Base Zechstein salt level (Figs. 4, 6b, and 7a-b) mainly developed after deposition of the Rotliegend Group, probably by reactivation of the Devonian structural grain as defined on the top acoustic basement level. The faults at the Base Zechstein salt level are generally basement-involved. A regional thickening trend of the sub-Rotliegend sequence I and the Rotliegend Group towards southwest within the Northern Permian Basin is reflected by the map in Fig. 9c.

6.5. Upper Permian-Triassic succession

Because the Lower Jurassic was deeply eroded during uplift associated with magmatism in the central North Sea, as expressed by the mid-Jurassic unconformity (Intra-Aalenian Unconformity; Underhill and Partington, 1993), the isochron map of the sequences bounded by the base of the Zechstein Group and the mid-Jurassic unconformity (Fig. 11a) is largely representing the upper Permian-Triassic succession in the study area. The isochron map reflects a gradual increase in thickness/accommodation space towards west and southwest. This was likely associated with a regional tilting of the area caused by uplift in the northeast/east and subsidence in the southwest/west. The maximum sediment thickness is inferred for the Hummer Graben with a maximum isochron value of 2.2 s (~4710 m using a 4285 m/s interval velocity in well 9/4–5).

The base of the Zechstein Group (base of the salt) is characterized by a strong seismic event (Fig. 4). The upper Permian Zechstein salt is

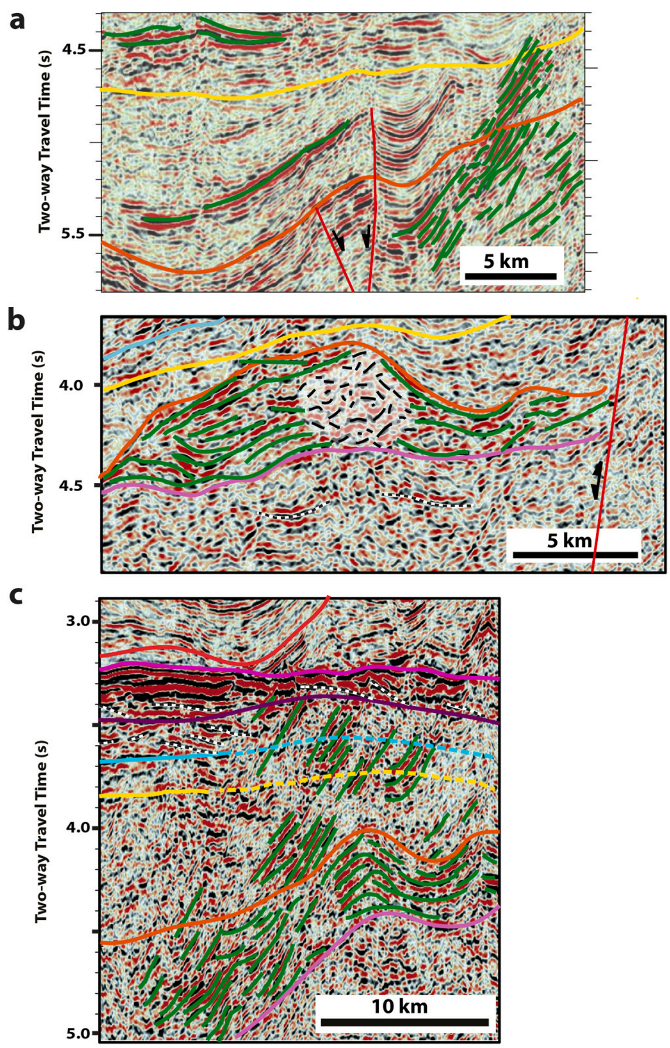

Fig. 8. Zoomed in view of the seismic profiles showing seismic facies comparable with intrusive magmatic features. a) zoomed in view of the seismic Fig. 7a showing intrusive related seismic facies units,b) zoomed in view of the seismic in Fig. 4, showing sill related seismic facies units (sill complex), c) zoomed in view of the seismic in Fig. 7d showing dyke related seismic facies cutting the sub-Rotliegend sequences and truncated by the Saalian Unconformity (i.e. Base Rotliegend).

widely distributed in the Northern Permian Basin, but it has been penetrated by wells in only a few occasions (e.g. wells 9/4–5, 11/5–1, 17/12–1, 17/12–1).

The Zechstein Group isochron map (Fig. 11b), which is expanding in overall thickness to the west and southwest of the study area, suggests that the primary salt succession gently thinned towards the Stavanger Platform, which likely coincides with the ancient margin of the Northern Permian Basin (Jackson and Lewis, 2013). It is therefore likely that the salt extended to the master fault that borders the Stavanger Platform. Towards the southeast, however, the salt is still present beyond the eastern and southeastern boundary faults of the Egersund Basin and stretches to the Lista Fault Blocks indicating that these faults were not barriers to salt deposition during the late Permian. Jackson and Lewis (2013) discussed that uneven distribution of salt on the hanging and foot wall of the Stavanger fault system shows a southward decrease of the SFS throw by the time of salt deposition, such that salt could onlap the footwall at lower elevations towards the south. With respect to the tectonic quietness during the ealy Permian, here we may argue that the faulting was slightly prior to or during salt deposition. It appears that some of the major N–S faults (e.g. the Krabbe and Hummer faults) were active in mid-late Permian time and affected the basin configuration and thickness distribution of salt. This is further supported by the recent extension of the Zechstein limit farther eastward across the Lista Fault Blocks into the Farsund Basin (Phillips et al., 2019).

Based on the seismic reflection configurations, the *Triassic* succession can be subdivided into a lower, a middle and an upper unit in the Hummer and Åsta grabens. The low amplitude middle Triassic unit is bounded by moderate and high amplitude units below and above, respectively. The lower Triassic unit displays thickness increase in the hanging walls of the Flekkefjord fault system and the Hummer Fault Zone (Fig. 12a) that indicate extensional faulting along the boundary faults of the graben. Deposition of the lower Triassic unit, combined with fault activity, may have contributed to triggering halokinesis. Accordingly, deposition in the Triassic was strongly influenced by halokinesis and the resulting local basins in rim synclines surrounding the salt structures. Sub-basins delineated by salt diapirs or salt walls were common (Figs. 4 and 7).

The rather uniform thickness of the middle Triassic sequence suggests limited tectonic or halokinetic influence in middle Triassic time. In contrast, the upper Triassic unit shows notable thinning in the center of the Hummer Graben and thickening adjacent to the Flekkefjord fault system (Fig. 12a). The base of the upper Triassic unit is an unconformity on which the internal reflections off-lap. This implies syn-tectonic deposition of the upper Triassic unit. The upper Triassic unit is unconformably overlain by the Middle Jurassic (or Lower Jurassic in deepest depositional settings, e.g. in the central Egersund Basin in wells 9/2–1 and 9/2-2, where the Lower Jurassic is at least partly preserved). The Hummer Fault Zone was soft-linked with the basement-involved segment during this phase (Fig. 12a).

The timing of movements along the Stavanger fault system cannot be determined with certainty because of erosion or non-deposition of the Triassic strata in the footwall. However, thickening of the Triassic strata in the immediate hanging wall of Stavanger fault system suggests that the fault system was active during the Triassic (Fig. 12b). At the southwestern margin of the Egersund Basin, however, more thickening of the Triassic strata in the hanging wall of the Egersund fault system shows that this fault system, compared to the Stavanger fault system, was relatively more active during the early Triassic. More details on the Triassic seismic stratigraphy and evolution of the Central North area, including the study area, are found in Jarsve et al. (2014a).

6.6. *Middle-Upper Jurassic sequence*

The Middle-Upper Jurassic sequence is bounded by the mid-Jurassic unconformity at its base and by the top of the Sauda Formation at its top (Fig. 3). The prominent reflection of the top Tau Formation divides this sequence into two distinctive seismic units based on amplitudes, with a high amplitude seismic facies unit overlain by a low amplitude one (Fig. 5). The reflection coincides with a sharp break in the well log data and characteristic seismic signature (i.e. low amplitude reflections with a negative high amplitude close to the top) due to an overall increasing-upward high organic carbon content (cf. Løseth et al., 2011) within the Tau Formation in the Egersund Basin area (Kalani et al., 2015a, b; Mannie et al., 2016; Mannie et al., 2014).

The lower seismic unit corresponds to the Middle and lowermost Upper Jurassic sequence (Bajocian-Kimmeridgian) comprising the Bryne, Sandnes, Egersund and Tau formations (cf. Mannie et al., 2016; Mannie et al., 2014), with a maximum thickness in the central Åsta Graben in the immediate hanging wall of the Sele High fault system (i.e. 0.6 s; Fig. 13a). Parts of the Egersund Basin did also subside during this time interval. The upper unit corresponds to the uppermost Jurassic Sauda Formation, which has its most distinct depocenter in the Egersund Basin (Fig. 13b). The Egersund Basin is positioned in the hanging wall of the Stavanger fault system (Fig. 13b). The Middle-Upper Jurassic has the geometry of a half-graben with maximum thickness adjacent to the fault documenting syn-tectonic deposition during the Middle-Late Jurassic.

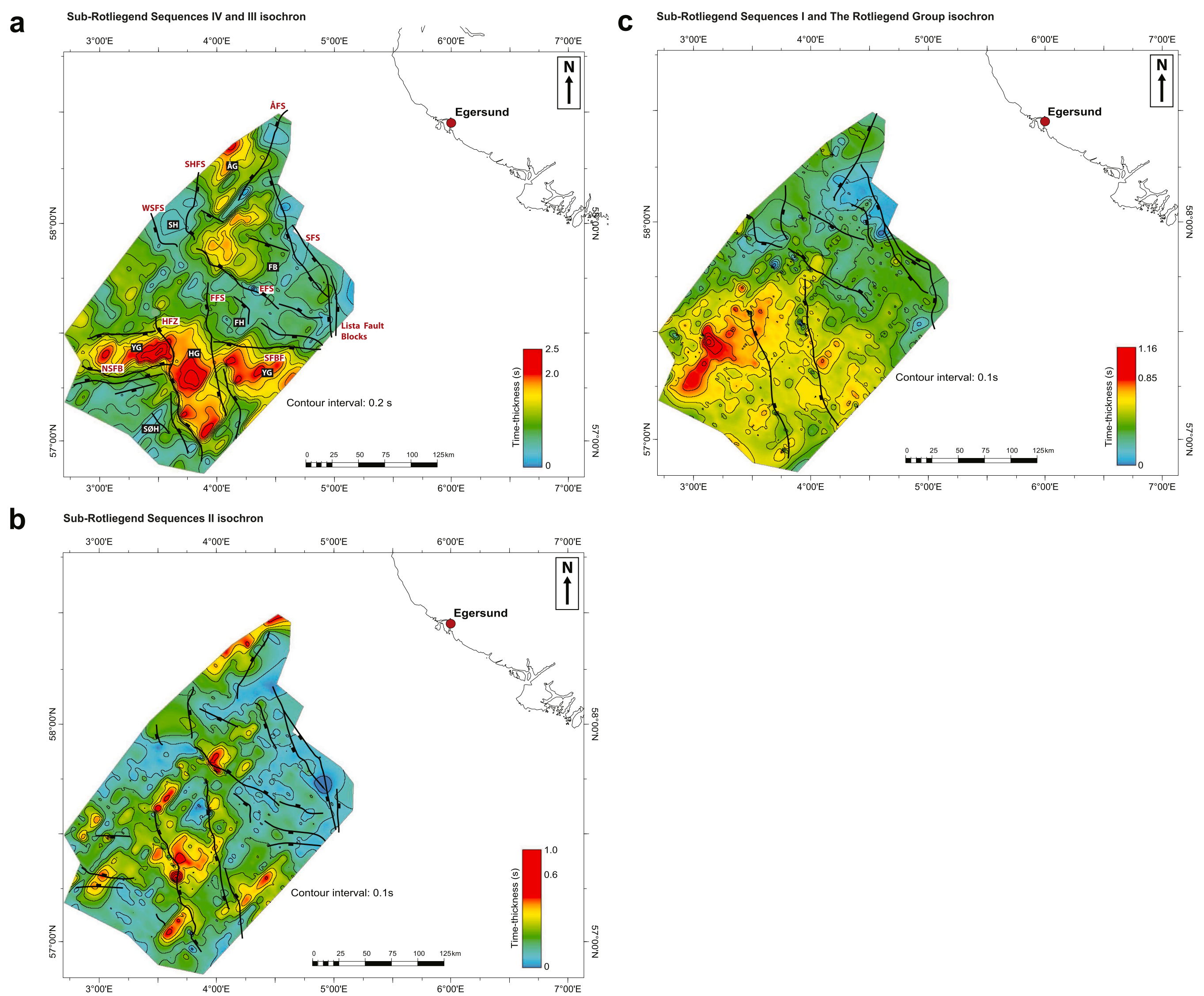

Fig. 9. Isochron maps of selected sub-salt stratigraphic units. Note that the trends aligned with the seismic grid are artefacts. (a) Isochron map of total sub-Rotliegend sequences IV and III showing the overall syn-rift configuration; (b) The isochron map of the sequence sub-Rotliegend II showing a sagged geometry configuration with maximum thicknesses beneath the Hummer Graben; (c) isochron map of total sub-Rotliegend sequence I and the Rotliegend showing the overall post-rift configuration. (For interpretation of the references to color in this figure, the reader is referred to the Web version of this article.)

The thickness changes of the Upper Jurassic are larger compared to that of the more coarse-grained Middle Jurassic deposits, suggesting more pronounced fault displacements during the Late Jurassic. The Egersund fault system had also control on the development of Egersund Basin during later parts of the Late Jurassic (Figs. 11b and 12b).

The hanging wall succession of the Åsta fault system shows prominent thickening of the Middle and lowermost Upper Jurassic in the Åsta Graben (Figs. 7e and 13a). Faulting ceased by latest Middle Jurassic time and the half-graben was subsequently drowned allowing the deposition of fine-grained sediments blanketing the faults of the Åsta fault system. This implies that the main phase of Jurassic faulting was earlier in the Åsta Graben than in the Egersund Basin.

Sediment depocenters developed during Middle Jurassic to Early Cretaceous were generally concurrent with those of the pre-Permian, except for the E-W striking elements (Figs. 13d and 14) demonstrating that the Jurassic-Early Cretaceous evolution of the Egersund Basin and its surrounding areas were likely influenced by the pre-Permian fault population and inhereted basement fabric.

Well 17/9-1 drilled Triassic sediments intruded by igneous rocks dated between 177 and 178 Ma. In the same well, nephelinitic lavas are found interbedded with the Lower Jurassic sedimentary strata and similarly show an age of 177–180 Ma (Furnes et al., 1982). Detailed interpretation of volcanic and magmatic evidences of Jurassic in the larger western Europe region is found in Van Bergen and Sissingh (2007), Latin et al. (1990) and Bergelin et al. (2011).

6.7. Lower Cretaceous sequence

The top of the Cromer Knoll Group defines the top of the lower Cretaceous, and is distinguished by a strong seismic reflection, which is due to the high acoustic impedance contrast with overlying chalk-dominated strata (Figs. 3 and 4).

The positions of the Lower Cretaceous depocenters (the Flekkefjord Formation and the Cromer Knoll Group) coincide with those of the Upper Jurassic (Fig. 13c). The maximum thickness is 1.1 s (~1570 m using a 2860 m/s interval velocity in well 9/2–1). The isochron map covering the interval from the mid-Jurassic unconformity to the top Lower Cretaceous is predominantly following depositional trends

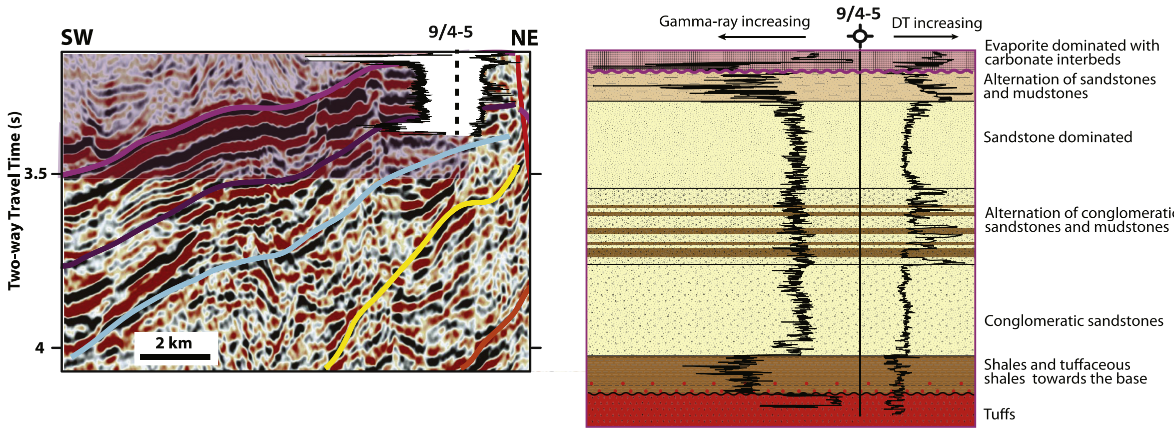

Fig. 10. (a) Part of the seismic section tied to well 9/4–5 showing seismic response of the Rotliegend and Sub-Rotliegend I-III sequences on the Flekkefjord High; (b) Lithology and well log response (gamma-ray and DT) of the Rotliegend Group underlain by tuffs of the Sub-Rotliegend I. For the colors assigned to the seismic sequence boundaries see Fig. 3. Seismic data courtesy of TGS. (For interpretation of the references to color in this figure, the reader is referred to the Web version of this article.)

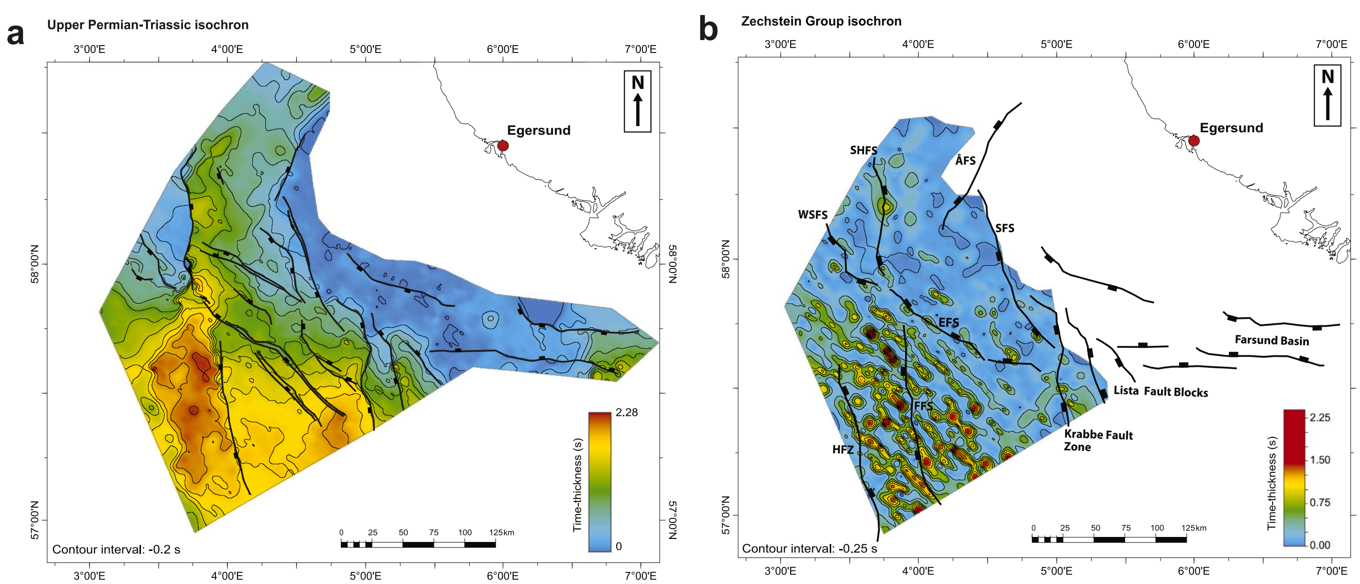

Fig. 11. (a) The Base Zechstein to mid-Jurassic unconformity isochron map. The map is largely representing the upper Permian-Triassic succession in the study area, and suggests a gentle depositional slope facing the west and southwest at this time; (b) The Zechstein isochron map. Salt succession thinned towards the Stavanger Platform. In the Egersund Basin, the salt extended to the master fault that borders the Stavanger Platform. Towards the southeast, the salt is still present beyond the eastern and south-eastern boundary faults of the Egersund Basin and stretches to the Lista Fault Blocks. (For interpretation of the references to color in this figure, the reader is referred to the Web version of this article.)

established in the Late Jurassic (Fig. 13d). To the east and southeast, a notable thickness of the Cromer Knoll Group was eroded due to the younger Cenozoic exhumation (Fig. 13c and d).

The main normal fault of the Stavanger fault system bounding the Egersund Basin terminates in the uppermost Lower Cretaceous (Fig. 12b). Here, a unit of uniform thickness covers both the hanging- and foot wall of the fault indicating that fault activity and associated differential subsidence had ceased, whereas for the Egersund fault system, faulting resulted in smaller thickness variations in the hanging wall (Fig. 12b). The N–S trending Hummer Fault Zone and Flekkefjord fault system show no signs of fault activity related to the continued rifting and subsidence in the adjacent Egersund Basin (Fig. 12a). Minor thickness variations across the Flekkefjord fault system and Hummer Fault Zone were likely related to salt withdrawal.

6.8. *Upper Cretaceous-Danian chalk group*

The chalk group shows thickening towards and onto the Stavanger Platform particularly in the northeast (Figs. 4 and 7). This thickening indicates that the chalk unit extended east of the present coastline prior to the Cenozoic uplift and erosion. Detailed discussion on the chalk thickness varitions in the North Sea including the Egersund Basin area can be found in Jarsve et al. (2014a). The geometry of the chalk unit indicates inversion of the Egersund Basin (Figs. 4, 7b and 12b) and the Åsta Graben (Fig. 7e) by reverse reactivation of the Stavanger fault system (cf. Jackson et al., 2013; Mogensen and Jensen, 1994; Phillips et al., 2016; Sørensen et al., 1992). Detailed analysis of growth strata in 3D seismic data reveal that the folds initiated with some diachroneity between latest Turonian and Santonian times and the anticline growth ceased in the Maastrichtian (Jackson et al., 2013). Locally, salt movements have played a role in the formation of some of the anticlines (Fig. 6d).

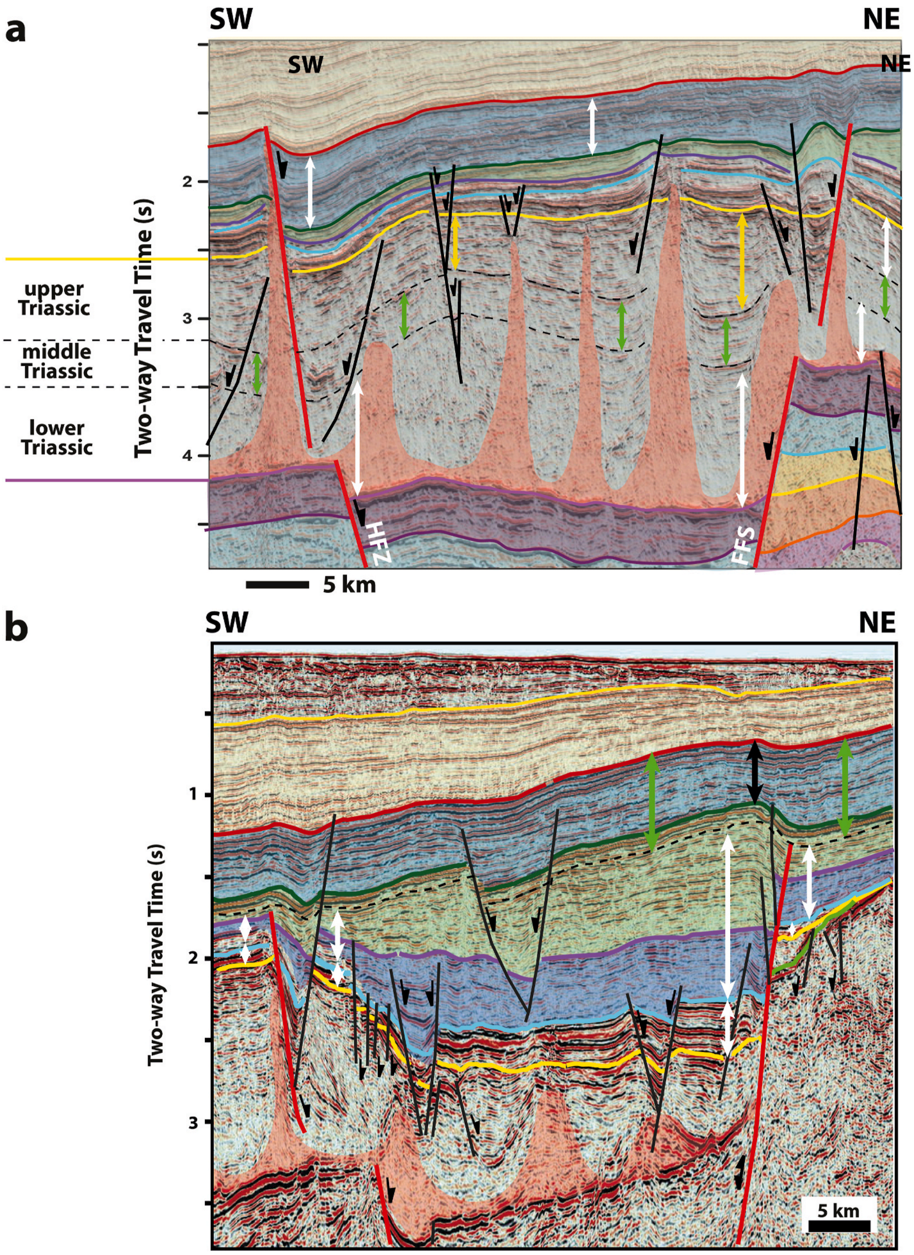

Fig. 12. Parts of seismic profile showing normal faulting and folding in the sub-basins of the larger Egersund Basin area: (a) The Hummer Graben, note the different thickness of the lower and upper Triassic units, and uniform thickness of the middle Triassic unit as marked by the white, yellow and green arrows, respectively; (b) the Egersund Basin, note the different time thicknesses as marked by white arrows, and uniform time thicknesses as marked by the green arrow. Abbreviations:. EFS - Egersund fault system, FFS - Flekkefjord fault system, HFZ - Hummer Fault Zone, SFS - Stavanger fault system, For the colors assigned to the seismic sequence boundaries and sequences see Fig. 3. Data courtesy of TGS. (For interpretation of the references to color in this figure, the reader is referred to the Web version of this article.)

6.9. *Cenozoic succession*

The Cenozoic succession shows a significant thickening and tilting towards central parts of the North Sea basin (Figs. 4 and 7). Thick sedimentary units prograded westwards from uplifted source areas in the northeast as recorded in NE-SW-oriented seismic profiles (Figs. 4 and 7, cf. Anell et al., 2009; Anell et al., 2012; Anell et al., 2010; Jarsve et al., 2014a, 2015). The uplift and tilting was initiated in the Oligocene mainly controlled by regional uplift and exposure of landmasses in southern Norway and concurrent basin subsidence in the central North Sea (Jarsve et al., 2015). The Egersund Basin was part of the uplifted area and exhumation has been estimated to increase across the basin from about 200 m in the southwest to 700–750 m in the northeast (Baig et al., 2019; Jensen and Schmidt, 1993; Kalani et al., 2015a).

7. Discussion

The present analysis particularly focuses on (1) the pre-Permian structural configuration and its relations to Caledonian and Variscan structuring, and the influence of pre-Permian structural grain on the post-Permian basin configuration; (2) the age of the deepest sedimentary sequences; (3) late Permian to early Triassic and middle Jurassic-early Cretaceous basin development; (4) the influence of the evaporite sequence on the linkage between the deep (sub-salt) and shallow (supra-salt) faults.

To illustrate the geological evolution of the Egersund Basin area, a map displaying positions of the active faults (surface fault traces) at various stratigraphic levels, and schematic cross-sections as interpreted from a NE-SW-profile are shown in Figs. 14 and 15, respectively. More regionally, the tectonic evolution of the larger central North area is presented in terms of a series of paleotectonic maps (Fig. 16).

7.1. *Pre-Permian sedimentation and structural grain*

The pre-Permian is characterized by an E-W structural grain, modified by a roughly N–S structural trend. This grain affects sub-Rotliegend

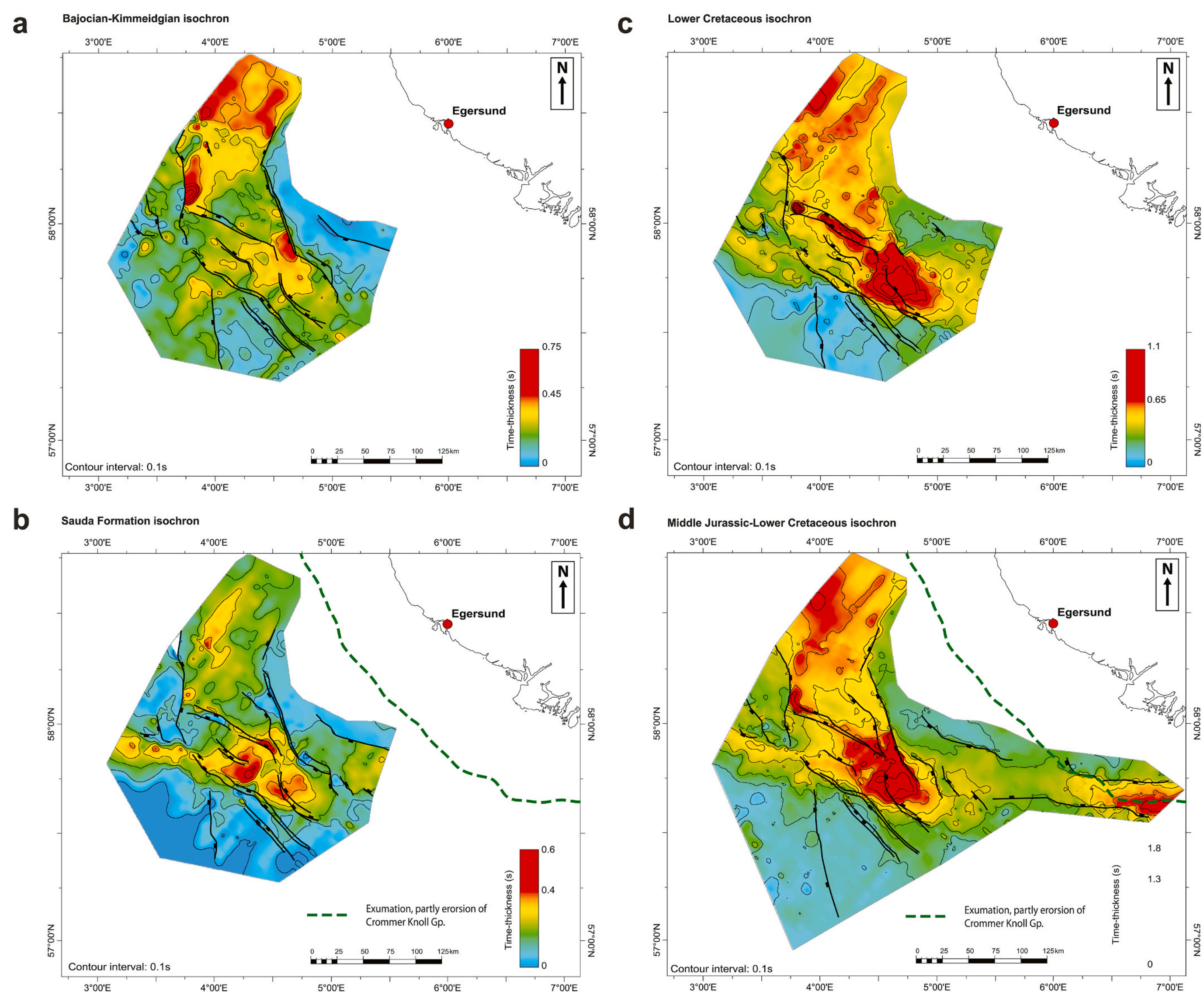

Fig. 13. a) Isochron maps of the Bajocian-Kimmeridgian Jurassic successions (i.e. bounded by the Mid-Jurassic unconformity at the base and the top Tau Formation to the top) showing the major Jurassic rifting stage; (b) Isochron map of the Sauda Formation; (c) Isochron map of the Lower Cretaceous; (d) Overall isochron map of the Middle Jurassic-Lower Cretaceous successions. (For interpretation of the references to color in this figure, the reader is referred to the Web version of this article.)

(pre-Permian) sequences IV and III (Figs. 14 and 15a). The sub-Rotliegend sequence IV is characterized by a chaotic reflection pattern above an unconformity (i.e. SRSB 4), likely representing the top of the acoustic basement. The structural grain is expressed as normal faults constraining elongated areas of sediment accumulation (Fig. 16a).

Parts of the assumed acoustic basement contain tilted stratified layers, for which radiometric datings suggest meta-sediments of Silurian (Farsund Basin) and Devonian (Sele High; wells 8/3–1 and 17/12–2) age, and these can be correlated with the Egersund Basin area (Marshall and Hewett, 2003). In the study area, the sub-Rotliegend sequences IV and III are underlain by the shallowly inclined basal decollement Devonian shear zone (Phillips et al., 2016) and overlain by the younger sub-Rotligend sequences (pre-Permian). Devonian basins with sandstone and conglomerates are also well known onshore on the western Norway mainland (e.g. Osmundsen and Andersen, 2001; Seranne and Seguret, 1987; Steel, 1976). A late Devonian-earliest Carboniferous age is therefore inferred for the E-W striking depocenters.

Reactivation of the WNW-ESE to NW-SE Tornquist trend (Cherry, 1993; Zanella and Coward, 2003) affecting the pre-Permian of the Egersund Basin area (Figs. 14, 15a and 16a) may have been associated with the construction and collapse of the Caledonian orogeny (Abramovitz and Thybo, 2000; Fossen, 2010; Fossen et al., 2014; Pegrum, 1984; Slagstad et al., 2011). The NNE-SSW and NNW-SSE structural grains may also contain elements of Caledonian origin (Andersson et al., 1996; Gabrielsen et al., 2002, 2018). Furthermore, a Variscan influence on the basement grain is also likely (e.g. Pegrum, 1984; Smit et al., 2016).

The NW-SE extention related to the Caledonain gravitational collapse, which was succeeded by late Devonian extension, is inferred to be oblique to both the E-W and N–S trends. Both fault systems are believed to have been active during the same tectonic phase tentatively dated to late Devonian-?early Carboniferous. From thickness variations and cross-cutting relationships it appears that the E-W structures became active slightly prior to the N–S structures. This may reflect that the extension direction had a larger angle to the E-W than to the N–S structural grains. The pre-Permian E-W faults bounding the Ytterbanken graben may have some deep-seated connection to the E-W faults bounding the Farsund Basin, which have been linked to several phases of movements along the Sorgenfrei-Tornquist Zone (Phillips et al., 2018). The E-W striking faults became inactive by the time of deposition of the sub-Rotliegend sequence II, becoming buried beneath this sequence. The E-W structures remained inactive during the further basin development

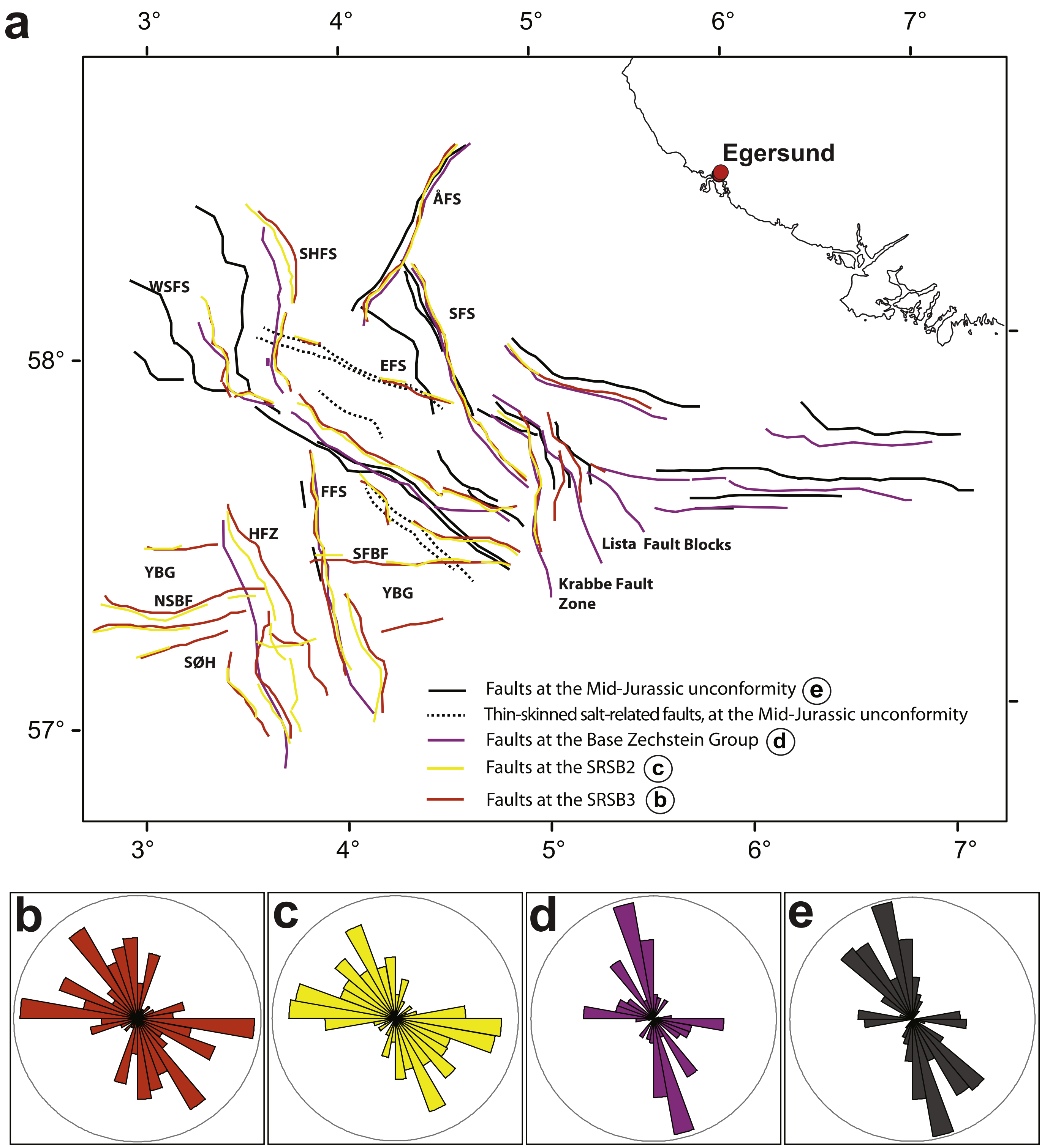

Fig. 14. Major normal fault systems interpreted at different stratigraphic levels. Abbreviations: ÅFS - Åsta fault set, EFS - Egersund fault system, FFS - Flekkefjord fault system, HFS - Hummer Fault Zone, NSBF - Northern Sørvestlandet High border fault, SFBF - Southern Flekkefjord High border fault, SFS - Stavanger fault system, SHFS - Sele High fault system, SØH - Sørvestlandet High, WSFS- West Sele fault system, YBG- Ytterbanken graben.

of the study area, suggesting a post-rift origin for sequence II.

7.2. Permian-Triassic basin development

The uniform thickness of the sub-Rotliegend sequence I and particularly the Rotliegend Group in the hanging and foot walls of the N–S and NW-SE trending master faults throughout the study area, reflect the lack of fault activity in this period (Fig. 15b). This is consistent with observations along the Sorgenfrei-Tornquist Zone elsewhere and within the Oslo Rift in Skagerrak where upper Carboniferous-lower Permian volcanics rest without any angular unconformity directly on Lower Paleozoic (Silurian) clastics deposited in the foreland basin of the Caledonides (Heeremans and Faleide, 2004).

The volcanic tuffs occurring in the sub-Rotliegend I sequence close to

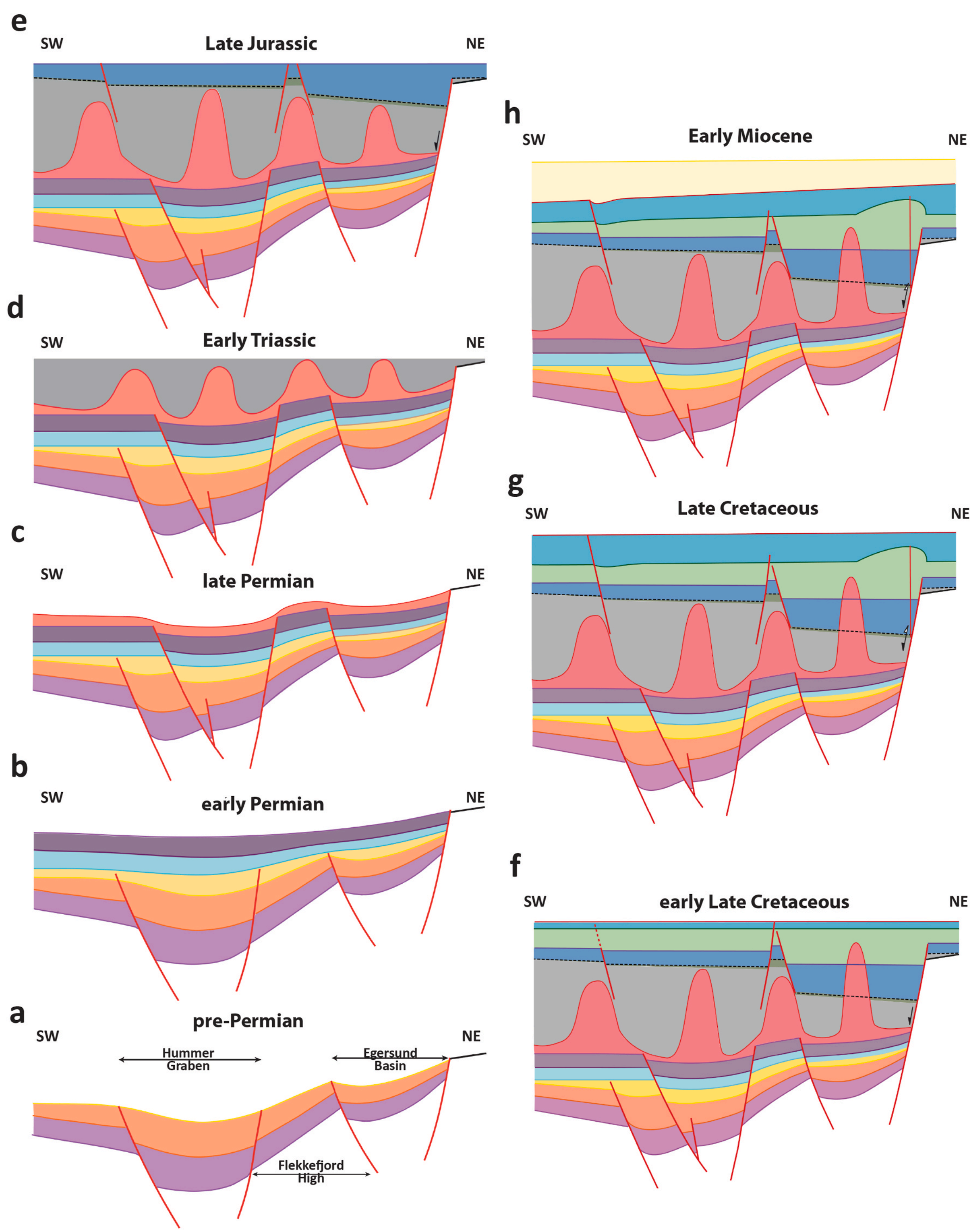

Fig. 15. Cartoons illustrating the pre-Permian present-day tectonic development within the Egersund Basin area. For the colors assigned to the seismic sequence boundaries and sequences see Fig. 3. a) The earliest stage of extension occurred in pre-Permian time in response to extensional tectonics involved with the Caledonian collapse; b) Uniform thickness of the Rotliegend Group throughout the study area, indicate minor syn-depositional faulting and likely limited extension in the Egersund Basin area during the early Permian; c) Active faulting during post-early Permian, during and/or after Zechstein salt deposition. Active faulting continued into the Early Triassic; d) During the Early Triassic, increased sedimentation rates from uplifted basin flanks contributed to the triggering of salt movements; e) During the Middle-Late Triassic accommodation space for deposition of clastic sediments was governed by the halokinesis. Thermal doming as inferred from the Mid-Jurassic unconformity was followed by a new phase of extension in late Middle Jurassic time; f) The Egersund Basin proper developed during the Late Jurassic-Early Cretaceous; g) In the Late Cretaceous, mild inversion along the northern flank of the Egersund Basin occurred; h) In the Cenozoic, regional tilting occurred and large depositional systems originated in the northeast prograded towards the basin centre. (For interpretation of the references to color in this figure, the reader is referred to the Web version of this article.)

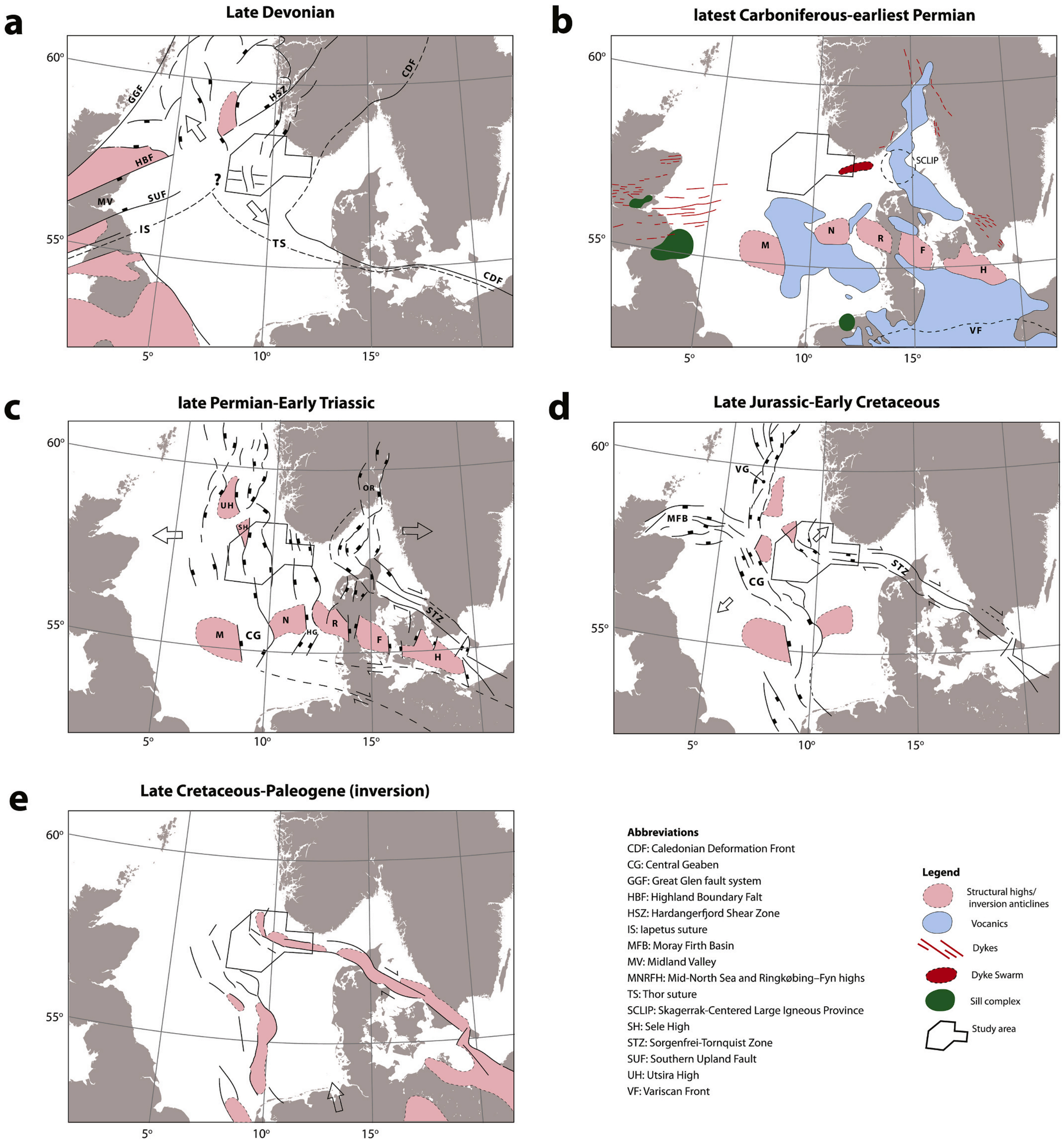

Fig. 16. Paleotectonic maps showing the evolution of the Egersund Basin in the larger Central North Sea area.

the Saalian Unconformity at the Carboniferous-Permian transition (e.g. well 9/4–5, Fig. 9) are likely affiliated with widespread magmatism dated around 300 Ma that is well known from northern Europe (Heeremans and Faleide, 2004; Timmerman et al., 2009). In the study area, it is suggested that the tuffs are associated with the intrusives, which most likely formed in the fracture networks developed by the late Carboniferous-arly Permian brittle reactivation of Devonian shear zones (cf. Lyngsie and Thybo, 2007; Phillips et al., 2016), reaching up to the Base of the Rotliegend Group (cf. Clausen et al., 2016). These intrusives likely belong to a dyke swarm which originated from a large igneous province centred in the Skagerrak area (Torsvik et al., 2008, Fig. 15b). This interpretation is supported by the inferred Carboniferous-Permian (296–300 Ma) dyke swarm recently addressed from the Farsund Basin (Phillips et al., 2017, Fig. 15b).

Absence of depocenters on the hanging wall of the Egersund Basin boundary faults (the Egersund and Stavanger fault systems) imply no E-W extensional tectonics during the late Permian- Triassic. Similarly in the Farsund Basin, Phillips et al. (2018) reported no signs of activity on the E-W trending faults bounding the basin. Further east, late Permian-Early Triassic dextral movements along the

Sorgenfrei-Tornquist Zone was taken up by the Oslo Rift through the Skagerrak Graben (Fig. 16c). Therefore it can be argued that during the late Permian-Early Triassic the Sorgenfrei-Tornquist Zone was not linked with the Farsund Basin, nor the Egersund Basin. In such a picture E-W extension on N–S trending faults affecting a wide area of the Central and Northern North Sea was mainly related to the Trans-European Fault and Elbe Line which were also reactivated with dextral movements in response to north-directed compression from the Variscan Orogeny in the south (e.g. Bartholomew et al., 1993).

The uniform thickness of the Rotliegend Group implies that the faults were active post-early Permian, i.e. during and/or after Zechstein salt deposition. Seismic data suggest that fault activity continued into the Early Triassic (Fig. 15d). The late Permian-Early Triassic faults were likely nucleated above basement faults (soft-linked for the Early Triassic segment). This is clearly the case for the boundary faults of the Hummer Graben (the Hummer Fault Zone and Flekkefjord fault system) because seismic profiles show a notable increase of the accommodation space on the hanging walls of the major normal fault systems like the Hummer Fault Zone, at the base of the Zechstein stratigraphic level. This means fault activity during salt deposition, and can be linked to the late Permian-Early Triassic extension (Fig. 15c and d).

While most of the inferred potential intrusives do not cross-cut the Rotliegend Group, a few do. These can be correlated with late Permian-Early Triassic igneous activity in western Norway (Færseth, 1978; Torsvik et al., 1997) and the Oslo Graben (Rasmussen et al., 1988; Sundvoll et al., 1990, 1992; Timmerman et al., 2009; Torsvik et al., 1998). Timmerman et al. (2009) suggested that minor igneous activities in the Oslo Graben were the result of regional extension around the Permian-Triassic transition (~250 Ma). Rift flank uplift and exhumation (Fossen et al., 2016) may have resulted in enhanced Early Triassic sediment supply, which may likely have triggered salt withdrawal in the central North Sea area (Fig. 14d) (Jarsve et al., 2014b).

To sum up, although the N–S structural grain may have had an older (basement) precursor, a subsequent set of normal faults became dominant in the study area during the late Permian-Early Triassic (Figs. 6b, 14 and 16c) reflecting a switch from NW-SE oriented stress regime related to Caledonian gravitional collaps and potentially following Devonian extension, to E-W directed extension during late Permian. Faulting continued during deposition of the Zechstein salt and affected the thickness distribution of the evaporites (Figs. 15c and 16c). This event was likely associated with dextral wrench movements along the Sorgenfrei-Tornquist Zone (Heeremans and Faleide, 2004).

7.3. Jurassic-Cretaceous basin development

Following a Triassic post-rift stage (e.g. Gabrielsen et al., 1990; Nøttvedt et al., 1995), E-W to NE-SW extension and associated sedimentation in the North Sea continued in the Jurassic (e.g. Færseth, 1996; Roberts et al., 1990, Fig. 16d).

The Egersund Basin proper formed during the late Jurassic in response to the same principal extension as the Central Graben and the Moray Firth. The predominant NW-SE striking array of normal faults is indicative of a NE-SW orientation of the least principle stress axis associated with the master faults in the Egersund Basin area (Figs. 13 and 14). The NW-SE orientation of the Middle Jurassic-Early Cretaceous depocentres is also in agreement with such a stress regime (Fig. 13). The Early Cretaceous development of the E-W trending depocenter in the Farsund Basin reflects renewed dextral strike-slip activity within the Sorgenfrei-Tornquist Zone at this time (cf. Mogensen and Korstgård, 2003; Pegrum, 1984; Phillips et al., 2018). This suggests that the transtensional activitites along the Sorgenfrei-Tornquist Zone were extended through the Farsund and Egersund basins during the Early Cretaceous (Fig. 16d). The maximum thickness of sediments was accommodated during Kimmeridgian-Tithonian times. That is why the deepest parts as displayed in the isochron map of the Sauda Formation coincide with the most developed configuration of the Egersund Basin (Fig. 13b).

During the Early Cretaceous, the Egersund Basin continued its development as a distinct basin until the later Early Cretaceous when the extension ceased (Fig. 15f). The Cromer Knoll Group isochron map (Fig. 11c) shows depocenters coincident with those of the Late Jurassic (Fig. 13a and b). The overall isochron map of the Mid-Jurassic unconformity to top Lower Cretaceous is predominantly following depositional trends resembling those of the Lower Cretaceous Cromer Knoll Group (Fig. 13c and d). However, as mentioned above the main development of the Egersund Basin to its present day configuration occurred during the Late Jurassic (i.e. as inferred from the Sauda Formation isochron map; Fig. 13c).

Reactivation by far-field Alpine compression during Late Cretaceous-Paleogene transpression resulted in inversion along the Sorgenfrei-Tornquist Zone continuing through the Farsund Basin to the Egersund Basin (Figs. 6d and 16e). In the Egersund Basin, inversion mainly affected the Stavanger fault system, causing mild inversion of the hanging wall of this segmented and basement-involved fault system (Figs. 6d, 15g and 16e; cf. Jackson et al., 2013). This resulted in sediments eroded in the northeast prograded towards the basin centre (Fig. 15h).

7.4. Coupling between faults at deep (sub-salt) and shallow (supra-salt) levels

Structural mapping shows varying conditions for fault linkage across the evaporite sequence. The master faults associated with the basin margins display different configurations, including soft-linking, firm-linking and hard-linking in the vertical dimension. Thus there are frequent examples that post-Rotliegend faults were soft-linked to basement faults. This is the case for the faults that were active at the earlier stages of the basin development during deposition of the sub-Rotliegend sequences IV and III in the Late Devonian?-Carboniferous (e.g. the Flekkefjord fault system, Egersund fault system, and Stavanger fault system). These were inactive during deposition of the sub-Rotliegend sequence I and particularly the Rotliegend Group (Figs. 4 and 7). In those cases the fault configurations are characterized by relatively stable basin margins. Such examples are also reported by other workers in vicinity of the present study area (e.g. Jackson and Lewis, 2013; Jackson et al., 2013; Tvedt et al., 2016).

It is well established that several factors such as evaporite thickness, overburden thickness, total fault displacement, extension rate and viscosity of evaporites play important roles in determining the coupling style between sub- and supra-salt structural faults (e.g. Jackson and Lewis, 2016; Jackson and Rotevatn, 2013; Koyi et al., 1993; Lewis et al., 2013; Stewart et al., 1997; Stewart et al., 1996).

Lewis et al. (2013), analyzing the Stavanger fault system, argued that the key control on style of coupling between sub- and supra-salt is presence of salt on the foot wall of the sub-salt fault. Accordingly, after deposition of the salt, supra-salt faults became soft-linked through the salt, transecting the salt sequence. Lewis et al. (2013) argued that the larger throw to the south of the Stavanger fault system enhanced the erosion of the foot wall by the time of the salt deposition which in turn, resulted in spreading the salt beyond the boundary fault. To the east and northeast in more marginal settings where the salt was not spread out beyond the hanging wall of the northern part of the Stavanger fault system and the Åsta fault system master faults, the sub- and supra-salt faults are hard-linked through the salt (Figs. 4 and 7). For example, presence of salt on the footwall of the pre-Permian master faults of the Hummer Fault Zone and Flekkefjord and Egersund fault systems possibly caused the soft-linked style of the sub- and supra-salt faults. In central parts of the study area, where the salt is thicker, faults are mostly segmented and soft-linked (Figs. 4 and 7). Thus, coupling of sub- and supra-salt segments of any certain fault within the Egersund Basin area, in our case, allows to consider them as coherent segments of the same fault (Lewis et al., 2013). Accordingly, with regard to reactivation of the fault systems during late Permian-Early Triassic and Middle Jurassic-late Early Cretaceous considering a partly shared strain between pre-Permian, late Permian-Early Triassic and Middle Jurassic-late Early Cretaceous is possible.

8. Conclusions

The configuration and geometry of the present Egersund Basin area is the result of multistage deformation where direction of extension has changed from dominantly NW-SE through E-W to NE-SW, involving dextral strike-slip movements. This development was to varying degree influenced by a basement structural grain (i.e. structural configuration and basement fabric), that likely included elements of Proterozoic and Caledonian origin. The influence of this grain was not surprisingly strongest on the oldest (sub-salt) and less so on the younger (supra-salt) sequences. The master faults that define the border zones of the major structural lows (basins) and highs reflects the basement grain to a large degree, whereas the faults with less offset have more diverse orientations. The long-lived Sorgenfrei-Tornquist Zone and the sub-paralell Trans-European Fault did also play important roles in the structuring of the Central North Sea area.

Late Devonian-?early Carboniferous NW-SE extension activated two sets of E-W and N–S trending faults bounding distinct pre-Permian depocenters. Tuffs tied to their associated seismic facies at the Carboniferous-Permian transition (≈300 Ma) can be linked to regional-scale rifting and volcanism, and may be associated with a large igneous province centred on the Skagerrak. Zechstein evaporites were deposited during early stages of the prominent late Permian-Early Triassic rift phase which affected a wider part of the central and northern North Sea. Mainly N–S trending faults were active in an E-W extensional regime. The Egersund Basin proper formed in the Middle-Late Jurassic as a result of regional extension across the North Sea and reactivation of the Sorgenfrei-Tornquist Zone which experienced a new phase of dextral movements. The spatial distribution and thickness of the Zechstein evaporites influenced extensively the vertical fault linkage and hence the position and geometry of the faults associated with the younger stages of the basin development.

CRediT authorship contribution statement

Mohsen Kalani: Investigation, Writing - original draft, Visualization. **Jan Inge Faleide:** Conceptualization, Methodology, Validation, Writing - review & editing, Supervision, Funding acquisition. **Roy Helge Gabrielsen:** Conceptualization, Methodology, Validation, Writing - review & editing, Supervision.

Declaration of competing interest

The authors declare that they have no known competing financial interests or personal relationships that could have appeared to influence the work reported in this paper.

Acknowledgements

This work was carried out within the CO2Seal project funded by Gassnova and Statoil through the Climit Programme of the Research Council of Norway. We thank TGS for making seismic data available and the IHS Markit for use of their IHS Kingdom seismic interpretation toolbox. Petrel of Sclumberger was used to produce seismic interpretation derived maps. Associate editor Tiago Alves is thanked for handling and commenting on the manuscript. Insightful comments and discussions by Thomas Phillips (Durham University), Kamaldeen Omosanya (NTNU, Norway) and an anonymous reviwer significantly improved the original manuscript. Ole Rønø Clausen (Aarhus University, Denmark) is also thanked for commenting on an arlier version of this work.

References

Abramovitz, T., Thybo, H., 1999. Pre-Zechstein structures around the MONA LISA deep seismic lines in the southern Horn Graben area. Bull. Geol. Soc. Den. 44, 99–116.

Abramovitz, T., Thybo, H., 2000. Seismic images of caledonian, lithosphere-scale collision structures in the southeastern North Sea along Mona Lisa profile 2. Tectonophysics 317, 27–54.

Andersson, M., Lie, J.E., Husebye, E.S., 1996. Tectonic setting of post-orogenic granites within SW Fennoscandia based on deep seismic and gravity data. Terra. Nova 8, 558–566.

Anell, I., Thybo, H., Artemieva, I.M., 2009. Cenozoic uplift and subsidence in the North Atlantic region: geological evidence revisited. Tectonophysics 474, 78–105.

Anell, I., Thybo, H., Rasmussen, E., 2012. A synthesis of cenozoic sedimentation in The north Sea. Basin Res. 24, 154–179.

Anell, I., Thybo, H., Stratford, W., 2010. Relating Cenozoic North Sea sediments to topography in southern Norway: the interplay between tectonics and climate. Earth Planet Sci. Lett. 300, 19–32.

Baig, I., Faleide, J.I., Mondol, N.H., Jahren, J., 2019. Burial and exhumation history controls on shale compaction and thermal maturity along the Norwegian North Sea basin margin areas. Mar. Petrol. Geol. 104, 61–85.

Banka, D., Pharaoh, T.C., Williamson, J.P., 2002. Potential field imaging of Palaeozoic orogenic structure in northern and central Europe. Tectonophysics 360, 23–45.

Bartholomew, I.D., Peters, J.M., Powell, C.M., 1993. Regional structural evolution of the North Sea: oblique slip and the reactivation of basement lineaments. In: Parker, J.R. (Ed.), Petroleum Geology Conference. The Geological Society, London, pp. 1109–1122.

Bergelin, I., Obst, K., Söderlund, U., Larsson, K., Johansson, L., 2011. Mesozoic rift magmatism in the North Sea region: 40Ar/39Ar geochronology of Scanian basalts and geochemical constraints. Int. J. Earth Sci. 100, 787–804.

Berthelsen, A., 1998. The Tornquist Zone northwest of the Carpathians: an intraplate pseudosuture. GFF 120, 223–230.

Bingen, B., Skår, Ø., Marker, M., Sigmond, E.M., Nordgulen, Ø., Ragnhildstveit, J., Mansfeld, J., Tucker, R.D., Liégeois, J.-P., 2005. Timing of continental building in the Sveconorwegian orogen, SW Scandinavia. Norwegian Journal of Geology/Norsk Geologisk Forening 85.

Blundell, D.J., Hobbs, R.W., Klemperer, S.L., Scottrobinson, R., Long, R.E., West, T.E., Duin, E., 1991. Crustal structure of the central and southern North Sea from BIRPS deep seismic reflection profiling. J. Geol. Soc. 148, 445–457.

Bruton, D.L., Gabrielsen, R.H., Larsen, B.T., 2010. The Caledonides of the Oslo Region, Norway–stratigraphy and structural elements. Norwegian J. Geol./Norsk Geologisk Forening 90, 93–121.

Cherry, S.T.J., 1993. The interaction of structure and sedimentary process controlling deposition of the upper jurassic brae formation conglomerate, block 16/17, North Sea. Geological Society, London, Petroleum Geology Conference series 4, 387–400.

Christiansson, P., Faleide, J.I., Berge, A.M., 2000. Crustal structure in the northern North Sea: an integrated geophysical study. Geological Society, London, Special Publications 167, 15–40.

Clausen, O.R., Andresen, K.J., Rasmussen, J.A., 2016. A Late Paleozoic sill complex and related paleo-topography in the eastern North Sea analyzed using 3D seismic data. Tectonophysics 674, 76–88.

Cocks, L.R.M., Fortey, R.A., 1982. Faunal evidence for oceanic separations in the Palaeozoic of Britain. J. Geol. Soc. (Lond.) 139, 465–478.

Corfu, F., Andersen, T.B., Gasser, D., 2014. The Scandinavian Caledonides: main features, conceptual advances and critical questions. Geological Society, London, Special Publications 390, 9–43.

Dixon, J.E., Fitton, J.G., Frost, R.T.C., 1981. The tectonic significance of post-carboniferous igneous activity in the North Sea. In: Illing, L.V., Hobson, G.C. (Eds.), Petroleum Geology of the Continental Shelf of North-West Europe. Heyden, London, pp. 121–137.

Donato, J.A., Tully, M.C., 1982. A proposed granite batholith along the western flank of the North Sea Viking Graben. Geophys. J. Roy. Astron. Soc. 69, 187–195.

Færseth, R., Gabrielsen, R.H., Hurich, C.A., 1995. Influence of basement in structuring of the North Sea Basin, offshore southwest Norway. Nor. Geol. Tidsskr. 75, 105–119.

Færseth, R.B., 1978. Mantle-derived lherzolite xenoliths and megacrysts from Permo-Triassic dykes, Sunnhordland, western Norway. Lithos 11, 23–35.

Færseth, R.B., 1996. Interaction of permo-triassic and jurassic extensional fault-blocks during the development of the Northern North Sea. J. Geol. Soc. 153, 931–944.

Fazlikhani, H., Fossen, H., Gawthorpe, R., Faleide, J.I., Bell, R.E., 2017. Basement structure and its influence on the structural configuration of the northern North Sea rift. Tectonics 36, 1151–1177.

Fjeldskaar, W., Prestholm, E., Guargena, C., Gravdal, N., 1993. Isostatic and tectonic development of the Egersund basin. In: Doré, A.G., Augustson, J.H., Hermanrud, C., Stewart, D.J., Sylta, Ø. (Eds.), Basin Modelling: Advances and Applications. Elsevier, Amsterdam, pp. 549–562.

Fossen, H., 1992. The role of extensional tectonics in the Caledonides of south Norway. J. Struct. Geol. 14, 1033–1046.

Fossen, H., 2010. Extensional tectonics in The north atlantic Caledonides: a regional view. In: Law, R.D., Butler, R.W.H., Holdsworth, R.E., Krabbendam, M., Strachan, R. A. (Eds.), Continental Tectonics and Mountain Building: the Legacy of Peach and Horne. The Geological Society (London), London, pp. 767–793.

Fossen, H., FazliKhani, H., Faleide, J.I., Ksienzyk, A.K., Dunlap, W.J., 2016. Post-caledonian Extension in the West Norway–northern North Sea Region: the Role of Structural Inheritance. Geological Society, London. Special Publications 439.

Fossen, H., Gabrielsen, R.H., Faleide, J.I., Hurich, C.A., 2014. Crustal stretching in the Scandinavian Caledonides as revealed by deep seismic data. Geology 42, 791–794.

Fossen, H., Hurich, C.A., 2005. The hardangerfjord shear zone in SW Norway and The north Sea: a large-scale low-angle shear zone in the caledonian crust. J. Geol. Soc. 162, 675–687.
Furnes, H., Elvsborg, A., Malm, O.A., 1982. Lower and middle jurassic alkaline magamatism in the Egersund Sub-basin, North Sea. Mar. Geol. 46, 53–69.
Gabrielsen, R., Færseth, R., Steel, R., Idil, S., Kløvjan, O., 1990. Architectural styles of basin fill in the northern Viking Graben. In: Blundell, D.J., Gibbs, A.D. (Eds.), Tectonic Evolution of the North Sea Rifts. Clarendon Press, Oxford, pp. 158–179.
Gabrielsen, R., Ramberg, I., 1979. Fracture patterns in Norway from LANDSAT imagery: results and potential use. In: Proceedings, Norwegian Sea Symposium, Tromsø, pp. 1–28.
Gabrielsen, R.H., 1984. Long-lived fault zones and their influence on the tectonic development of the southwestern Barents Sea. J. Geol. Soc. 141, 651–662.
Gabrielsen, R.H., Braathen, A., Dehls, J., Roberts, D., 2002. Tectonic lineaments of Norway. Norw. J. Geol. 82, 153-117 154.
Gabrielsen, R.H., Færseth, R., Hamar, G., Rønnevik, H., 1984. Nomenclature of the main structural features on the Norwegian Continental Shelf north of the 62nd parallel. In: Spencer, A.M. (Ed.), Petroleum Geology of the North European Margin: Proceedings of the North European Margin Symposium (NEMS '83), Organized by the Norwegian Petroleum Society and Held at the Norwegian Institute of Technology (NTH) in Trondheim 9–11 May, 1983. Graham & Trotman, London, pp. 41–60.
Gabrielsen, R.H., Fossen, H., Faleide, J.I., Hurich, C.A., 2015. Mega-scale Moho relief and the structure of the lithosphere on the eastern flank of the Viking Graben, offshore southwestern Norway. Tectonics 34, 2014TC003778.
Gabrielsen, R.H., Nystuen, J.P., Olesen, O., 2018. Fault distribution in the precambrian basement of south Norway. J. Struct. Geol. 269–289.
Hansen, D.M., Cartwright, J., 2006. Saucer-shaped sill with lobate morphology revealed by 3D seismic data: implications for resolving a shallow-level sill emplacement mechanism. J. Geol. Soc. 163, 509–523.
Harland, W.B., 1969. Contribution of spitsbergen to understanding of tectonic evolution of north atlantic region: chapter 58: arctic regions. In: Kay, M. (Ed.), North Atlantic - Geology and Continental Drift, vol. 12. AAPG Memoir, pp. 817–851.
Heeremans, M., Faleide, J., 2004. Permo-Carboniferous Rifting in the Skagerrak, Kattegat and the North Sea: Evidence from Seismic and Borehole Data. Permo-Carboniferous Rifting in Europe, vol. 223. Geological Society Special Publication, pp. 159–177.
IHS, 2013. Release Notes for IHS Kingdom Software Version 8.8 Service Pack 1. http://downloads.seismicmicro.com/servicepak/TKS_88_SP1_ReadMe.pdf. (Accessed 22 April 2013).
Irwin, H., Hermanrud, C., Carlsen, E., Vollset, J., Nordvall, I., 1993. Basin modelling of hydrocarbon charge in the Egersund basin, Norwegian North Sea, pre-and post-drilling assessments. In: Doré, A.G., Augustson, J.H., Hermanrud, C., Stewart, D.J., Sylta, Ø. (Eds.), Basin Modelling: Advances and Applications. Elsevier, Amsterdam, pp. 539–548.
Jackson, C.A.L., Chua, S.T., Bell, R.E., Magee, C., 2013. Structural style and early stage growth of inversion structures: 3D seismic insights from the Egersund Basin, offshore Norway. J. Struct. Geol. 46, 167–185.
Jackson, C.A.L., Lewis, M.M., 2013. Physiography of the NE margin of the permian Salt Basin: new insights from 3D seismic reflection data. J. Geol. Soc. 120, 857–860.
Jackson, C.A.L., Lewis, M.M., 2016. Structural style and evolution of a salt-influenced rift basin margin; the impact of variations in salt composition and the role of polyphase extension. Basin Res. 28, 81–102.
Jackson, C.A.L., Rotevatn, A., 2013. 3D seismic analysis of the structure and evolution of a salt-influenced normal fault zone: a test of competing fault growth models. J. Struct. Geol. 54, 215–234.
Jarsve, E.M., Eidvin, T., Nystuen, J.P., Faleide, J.I., Gabrielsen, R.H., Thyberg, B.I., 2015. The Oligocene succession in the eastern North Sea: basin development and depositional systems. Geol. Mag. 152, 668–693.
Jarsve, E.M., Faleide, J.I., Gabrielsen, R.H., Nystuen, J.P., 2014a. Mesozoic and cenozoic basin configurations in The north Sea, chapter 15. In: Martinius, A.W., Ravnås, R., Howell, J.A., Steel, R.J., Wonham, J.P. (Eds.), From Depositional Systems to Sedimentary Successions on Norwegian Continental Margin. Wiley-Blackwell, pp. 417–452.
Jarsve, E.M., Maast, T.E., Gabrielsen, R.H., Faleide, J.I., Nystuen, J.P., Sassier, C., 2014b. Seismic stratigraphic subdivision of the Triassic succession in the Central North Sea; integrating seismic reflection and well data. J. Geol. Soc. (Lond.) 353–374.
Jensen, L.N., Schmidt, B.J., 1993. Neogene uplift and erosion offshore south Norway: magnitude and consequences for hydrocarbon exploration in the Farsund Basin. In: Spencer, A. (Ed.), Generation, Accumulation and Production of Europe's Hydrocarbons III. Springer Berlin Heidelberg, pp. 79–88.
Kalani, M., Jahren, J., Mondol, N.H., Faleide, J.I., 2015a. Compaction processes and rock properties in uplifted clay dominated units, - the Egersund Basin, Norwegian North Sea. Mar. Petrol. Geol. 68, 596–613.
Kalani, M., Jahren, J., Mondol, N.H., Faleide, J.I., 2015b. Petrophysical implications of source rock microfracturing. Int. J. Coal Geol. 143, 43–67.
Klemperer, S.L., 1988. Crustal thinning and nature of extension in the northern North Sea from deep seismic reflection profiling. Tectonics 7, 803–821.
Klemperer, S.L., Hurich, C.A., 1990. Lithosphere structure of the North Sea from deep seismic reflection profiling. In: Blundell, D.J., Gibbs, A.D. (Eds.), Tectonic Evolution of the North Sea Rifts. Clarendon Press, Oxford, pp. 37–63.
Koyi, H., Jenyon, M., Petersen, K., 1993. The effect of basement faulting on diapirism. J. Petrol. Geol. 16, 285–312.
Lassen, A., Thybo, H., 2012. Neoproterozoic and Palaeozoic evolution of SW Scandinavia based on integrated seismic interpretation. Precambrian Res. 204– 205, 75–104.
Latin, D., Dixon, J., White, N., Fitton, J., 1990. Mesozoic magmatic activity in the North Sea Basin: implications for stretching history. In: Hardman, R., Brooks, J. (Eds.), Tectonic Events Responsible for Britains's Oil and Gas Reserves. Geological Society Special Publications, pp. 207–227.
Lewis, M.M., Jackson, C.A.L., Gawthorpe, R.L., 2013. Salt-influenced normal fault growth and forced folding: the Stavanger fault system, North Sea. J. Struct. Geol. 54, 156–173.
Løseth, H., Wensaas, L., Gading, M., Duffaut, K., Springer, M., 2011. Can hydrocarbon source rocks be identified on seismic data? Geology 39, 1167–1170.
Lyngsie, S.B., Thybo, H., 2007. A new tectonic model for the Laurentia−Avalonia−Baltica sutures in the North Sea: a case study along MONA LISA profile 3. Tectonophysics 429, 201–227.
Magee, C., Hunt-Stewart, E., Jackson, C.A.L., 2013. Volcano growth mechanisms and the role of sub-volcanic intrusions: insights from2Dseismic reflection data. Earth Planet Sci. Lett. 373, 41–53.
Mannie, A.S., Jackson, C.A.-L., Hampson, G.J., Fraser, A.J., 2016. Tectonic controls on the spatial distribution and stratigraphic architecture of a net-transgressive shallow-marine synrift succession in a salt-influenced rift basin: middle to Upper Jurassic, Norwegian Central North Sea. J. Geol. Soc. 173, 901–915.
Mannie, A.S., Jackson, C.A.L., Hampson, G.J., 2014. Structural controls on the stratigraphic architectureof net-transgressive shallow-marine strata in a salt-influenced rift basin: middle-to-Upper Jurassic Egersund Basin, Norwegian North Sea. Basin Res. 26, 1–26.
Marshall, J.E.A., Hewett, A.J., 2003. Devonian. In: Evans, D., Graham, C., Armour, A., Bathurst, P. (Eds.), The Millennium Atlas: Petroleum Geology of the Central and Northern North Sea. Geological Society (London), London, UK, pp. 65–81.
Maystrenko, Y.P., Scheck-Wenderoth, M., 2013. 3D lithosphere-scale density model of the Central European Basin System and adjacent areas. Tectonophysics 601, 53–77.
Mogensen, T., Korstgård, J., 2003. Triassic and jurassic transtension along part of the sorgenfrei-tornquist zone, in the Danish kattegat. In: Ineson, J.R., Surlyk, F. (Eds.), The Jurassic of Denmark and Greenland, vol. 1. Geological Survey of Denmark and Greenland Bulletin, pp. 439–458.
Mogensen, T.E., Jensen, L.N., 1994. Cretaceous subsidence and inversion along the tornquist zone from kattegat to the Egersund basin, 12. First Break, pp. 211–222.
Myhre, L., 1975. Lithology. Well No 8/3-1, NPD Paper. Norwegian Petroleum Directoriate, Stavanger, p. 20.
Nøttvedt, A., Gabrielsen, R., Steel, R., 1995. Tectonostratigraphy and sedimentary architecture of rift basins, with reference to the northern North Sea. Mar. Petrol. Geol. 12, 881–901.
NPD, 2016. http://factpages.npd.no/factpage..
Nystuen, J.P., 1989. Rules and Recommendations for Naming Geological Units in Norway by the Norwegian Committee on Stratigraphy. Norsk Geologisk Tidsskrift, p. 110.
Odinsen, T., Reemst, P., Beek, P.V.D., Faleide, J.I., Gabrielsen, R.H., 2000. Permo-Triassic and Jurassic extension in the northern North Sea: results from tectonostratigraphic forward modelling. Geological Society, London, Special Publications 167, 83–103.
Osmundsen, P.T., Andersen, T.B., 2001. The Middle Devonian basins of western Norway; sedimentary response to large-scale transtensional tectonics? Tectonophysics 332, 51–68.
Pegrum, R.M., 1984. The extension of the tornquist zone in the Norwegian North Sea. GFF 106, 394–395.
Pharaoh, T.C., 1999. Palaeozoic terranes and their lithospheric boundaries within the Trans-European Suture Zone (TESZ): a review. Tectonophysics 314, 17–41.
Phillips, T., Jackson, C.A.-L., Bell, R., Valencia, A., 2019. Rivers, Reefs, and Deltas; Geomorphological Evolution of the Jurassic of the Farsund Basin, Offshore Southern Norway. Petroleum Geoscience petgeo2018-2056.
Phillips, T.B., Jackson, C.A.L., Bell, R.E., Duffy, O.B., 2018. Oblique reactivation of lithosphere-scale lineaments controls rift physiography – the upper-crustal expression of the Sorgenfrei–Tornquist Zone, offshore southern Norway. Solid Earth 9, 403–429.
Phillips, T.B., Jackson, C.A.L., Bell, R.E., Duffy, O.B., Fossen, H., 2016. Reactivation of intrabasement structures during rifting: a case study from offshore southern Norway. J. Struct. Geol. 91, 54–73.
Phillips, T.B., Magee, C., Jackson, C.A.-L., Bell, R.E., 2017. Determining the three-dimensional geometry of a dike swarm and its impact on later rift geometry using seismic reflection data. Geology 46, 119–122.
Planke, S., Rasmussen, T., Rey, S.S., Myklebust, R., 2005. Seismic characteristics of volcanic intrusions and hydrpthermal vent complexes in Vøring and Møring basins. In: Doré, A.G., Vining, B.A. (Eds.), Petroleum Geology: North-West Europe and Global Perspectives- Proceeding of the 6th Petroleum Geology Conference. The Geological Society (London), London, pp. 833–844.
Planke, S., Symonds, P.A., Alvestad, E., Skogseid, J., 2000. Seismic volcanostratigraphy of large-volume basaltic extrusive complexes on rifted margins. J. Geophys. Res. 105, 19335–19351.
Rasmussen, E., Neumann, E., Andersen, T., Sundvoll, B., Fjerdingstad, V., Stabel, A., 1988. Petrogenetic processes associated with intermediate and silicic magmatism in the Oslo rift, south-east Norway. Mineral. Mag. 52, 293-207.
Reeve, M.T., Bell, R.E., Jackson, C.A.-L., 2014. Origin and significance of intra-basement seismic reflections offshore western Norway. J. Geol. Soc. 171, 1–4.
Rey, P., Burg, J.-P., Casey, M., 1997. The Scandinavian Caledonides and their relationship to the Variscan belt. Geological Society, London, Special Publications 121, 179–200.
Roberts, A.M., Yielding, G., Badley, M.E., 1990. A kinematic model for the orthogonal opening of the late Jurassic North Sea rift system, Denmark-Mid Norway. In: Blundell, D.J., Gibbs, A.D. (Eds.), Tectonic Evolution of the North Sea Rifts. Oxford University Press, Oxford, UK.

Roberts, D., 2003. The Scandinavian Caledonides: event chronology, palaeogeographic settings and likely modern analogues. Tectonophysics 365, 283–299.

Rocchi, S., Mazzotti, A., Marroni, M., Pandolfi, L., Costantini, P., Giuseppe, B., Biase, D. d., Federici, F., Lô, P.G., 2007. Detection of Miocene saucer-shaped sills (offshore Senegal) via integrated interpretation of seismic, magnetic and gravity data. Terra. Nova 19, 232–239.

Seranne, M., Seguret, M., 1987. The Devonian basins of western Norway: tectonics and kinematics of an extending crust. Geological Society, London, Special Publications 28, 537–548.

Slagstad, T., Davidsen, B., Daly, J.S., 2011. Age and composition of crystalline basement rocks on the Norwegian continental margin: offshore extension and continuity of the Caledonian-Appalachian orogenic belt. Journal of the Geological Society of London 168, 1167–1185.

Smethurst, M.A., 2000. Land–offshore tectonic links in western Norway and the northern North Sea. J. Geol. Soc. 157, 769–781.

Smit, J., van Wees, J.-D., Cloetingh, S., 2016. The Thor suture zone: from subduction to intraplate basin setting. Geology 44, 707–710.

Sørensen, S., Morizot, H., Skottheim, S., 1992. A tectonostratigraphic analysis of the southeast Norwegian North Sea Basin. In: Larsen, R.M., Brekke, H., Larsen, B.T., Talleraas, E. (Eds.), Structural and Tectonic Modelling and its Application to Petroleum Geology. Elsevier, Amsterdam, pp. 19–42.

Steel, R.J., 1976. Devonian basins of western Norway-sedimentary response to tectonism and to varying tectonic context. Tectonophysics 36, 207–224.

Stewart, I.J., Rattey, R.P., Vann, I.R., 1992. Structural style and the habitat of hydrocarbons in the North Sea. In: Larsen, R.M., Brekke, H., Larsen, B.T., Talleraas, E. (Eds.), Structural and Tectonic Modelling and its Application to Petroleum Geology. Elsevier, Amsterdam, pp. 197–220.

Stewart, S., Ruffell, A., Harvey, M., 1997. Relationship between basement-linked and gravity-driven fault systems in the UKCS salt basins. Mar. Petrol. Geol. 14, 581–604.

Stewart, S.A., Harvey, M.J., Otto, S.C., Weston, P.J., 1996. Influence of salt on fault geometry: examples from the UK salt basins. Geological Society, London, Special Publications 100, 175–202.

Sundvoll, B., Larsen, B.T., Wandaas, B., 1992. Early magmatic phase in the Oslo Rift and its related stress regime. Tectonophysics 208, 37–54.

Sundvoll, B., Neumann, E.R., Larsen, B.T., Tuen, E., 1990. Age relations among Oslo Rift magmatic rocks: implications for tectonic and magmatic modelling. Tectonophysics 178, 67–87.

Thybo, H., 2001. Crustal structure along the EGT profile across the Tornquist Fan interpreted from seismic, gravity and magnetic data. Tectonophysics 334, 155–190.

Timmerman, M.J., Heeremans, M., Kirstein, L.A., Larsen, B.T., Spencer-Dunworth, E.-A., Sundvoll, B., 2009. Linking changes in tectonic style with magmatism in northern Europe during the late Carboniferous to latest Permian. Tectonophysics 473, 375–390.

Torsvik, T.H., Andersen, T.B., Eide, E.A., Walderhaug, H.J., 1997. The age and tectonic significance of dolerite dykes in western Norway. J. Geol. Soc. 154, 961–973.

Torsvik, T.H., Cocks, L.R.M., 2016. Earth History and Palaeogeography. Cambridge University Press.

Torsvik, T.H., Eide, E.A., Meert, J.G., Smethurst, M.A., Walderhaug, H.J., 1998. The Oslo Rift: new palaeomagnetic and 40Ar/39Ar age constraints. Geophys. J. Int. 135, 1045–1059.

Torsvik, T.H., Smethurst, M.A., Burke, K., Steinberger, B., 2008. Long term stability in deep mantle structure: evidence from the ~300 Ma skagerrak-centered large igneous province (the SCLIP). Earth Planet Sci. Lett. 267, 444–452.

Tvedt, A.B.M., Rotevatn, A., Jackson, C.A.L., 2016. Supra-salt normal fault growth during the rise and fall of a diapir: Perspectives from 3D seismic reflection data, Norwegian North Sea. J. Struct. Geol. 91, 1–26.

Underhill, J.R., Partington, M.A., 1993. Jurassic thermal doming and deflation in the North Sea: implications of the sequence stratigraphic evidence. In: Petroleum Geology Conference Series. Geological Society, London, pp. 337–345.

Van Bergen, M., Sissingh, W., 2007. Magmatism in The Netherlands: expression of the north-west European rifting history. In: Wong, T.E., Batjes, D.A.J., Jager, J.d. (Eds.), Geology of the Netherlands. Royal Netherlands Academy of Arts and Sciences, Amsterdam, pp. 197–221.

Zanella, E., Coward, M.P., 2003. Structural framework. In: Evans, D., Graham, C., Armour, A., Bathurst, P. (Eds.), Millennium Atlas: Petroleum Geology of the Central and Northern North Sea CD. Geological Society, London, pp. 45–59.

Ziegler, P., 1990. Tectonic and Palaeogeographic Development of the North Sea Rift System. Tectonic evolution of the North Sea rifts, pp. 1–36.